10-2-2015

Evidence that the DNA mismatch repair system removes 1-nucleotide Okazaki fragment flaps.

Lyudmila Y Kadyrova

Basanta K Dahal

Farid A Kadyrov

Recommended Citation
Kadyrova, Lyudmila Y, Dahal, Basanta K and Kadyrov, Farid A. "Evidence that the DNA mismatch repair system removes 1-nucleotide Okazaki fragment flaps.." *The Journal of Biological Chemistry* 290, No. 40 (Oct 2015): 24051-24065. doi:10.1074/jbc.M115.660357.

Evidence that the DNA Mismatch Repair System Removes 1-nt Okazaki Fragment Flaps*

Lyudmila Y. Kadyrova, Basanta K. Dahal, and Farid A. Kadyrov[1]

[1]From the Department of Biochemistry and Molecular Biology, Southern Illinois University School of Medicine, Carbondale, IL 62901, USA.

*Running title: *The MMR system and Okazaki fragment maturation*

To whom correspondence should be addressed: Farid Kadyrov, Department of Biochemistry and Molecular Biology, Southern Illinois University School of Medicine, Carbondale, IL 62901, USA, Tel.: (618) 453-6405; e-mail: fkadyrov@siumed.edu

Keywords: Genomic instability, cancer, DNA mismatch repair, mutL homolog 1 (MLH1), DNA endonuclease, DNA replication, Okazaki fragment maturation.

Background: The DNA mismatch repair (MMR) system protects humans from cancer.
Results: Combining an MMR system defect (*msh2*Δ) with *rad27*Δ causes a strong synergistic increase in the rate of 1-bp insertions and a reconstituted MMR system removes 1-nt flaps.
Conclusion: The MMR system removes 1-nt Okazaki fragment flaps.
Significance: A new function of the MMR system was identified.

ABSTRACT

The MMR system plays a major role in promoting genome stability and suppressing carcinogenesis. In this work, we investigated whether the MMR system is involved in Okazaki fragment maturation. We found that in the yeast *Saccharomyces cerevisiae* the MMR system and the flap endonuclease Rad27 act in overlapping pathways that protect the nuclear genome from 1-bp insertions. In addition, we determined that purified yeast and human MutSα proteins recognize 1-nt DNA and RNA flaps. In reconstituted human systems, MutSα, PCNA, and RFC activate MutLα endonuclease to remove the flaps. ATPase and endonuclease mutants of MutLα are defective in the flap removal. These results suggest that the MMR system contributes to the removal of 1-nt Okazaki fragment flaps.

INTRODUCTION

Genome stability is essential for maintaining life and preventing numerous genetic disorders. The MMR system promotes genome stability by correcting replicative DNA polymerase errors, removing mismatches formed during homologous recombination, impeding homeologous recombination, and participating in DNA damage response (1-5). Genetic or epigenetic inactivation of the MMR system strongly predisposes humans to several types of cancers (6). MMR has been extensively studied in *E. coli* and eukaryotes (7,8).

MutLα (MLH1-PMS2 heterodimer in humans and MLH1-PMS1 heterodimer in yeast), MutSα (MSH2-MSH6 heterodimer), MutSβ (MSH2-MSH3 heterodimer), EXO1, PCNA, and RFC are the key eukaryotic MMR factors (9-23). Eukaryotic MMR occurs both on the leading and lagging strands, but mismatches on the lagging strands are corrected more efficiently than those on the leading strands (24). The first step in eukaryotic MMR is recognition of the mismatch by the MutS homolog MutSα or MutSβ (11,12,15,19). After mismatch recognition, MutSα or MutSβ and loaded PCNA activate MutLα to incise the discontinuous daughter strand in the

vicinity of the mismatch (25-28). The endonuclease activity of MutLα depends on the integrity of its ATPase sites and the DQHA$(X)_2$E$(X)_4$E motif (25,26). A strand break generated by MutLα 5′ to the mismatch serves as the entry site for MutSα-activated Exonuclease 1 to degrade a mismatch-containing segment of the daughter strand in a 5′→3′ excision reaction (21,25). The resulting gap is repaired by DNA polymerase δ holoenzyme (29). The loss of Exonuclease 1 causes only a modest MMR defect in yeast and mice (18,22). Consistent with these observations, a reconstituted system lacking Exonuclease 1 is proficient in MMR (30). The reconstituted system bypasses the requirement for Exonuclease 1 in the mismatch removal by relying on the strand-displacement activity of DNA polymerase δ holoenzyme.

In addition to mismatches, several other aberrant structures with significant mutagenic potential are formed during DNA replication. Among them are Okazaki fragment flaps (31,32). Okazaki fragment maturation is a process that removes the flaps and joins the trimmed ends together producing continuous strands (33,34). Genetic evidence indicates that defective removal of Okazaki fragments flaps causes genome instability (31,32). In eukaryotes, Rad27/FEN1 endonuclease, Dna2 helicase/nuclease, and the 3′→5′ exonuclease activity of DNA polymerase δ remove Okazaki fragment flaps (32-36). PCNA interacts with Rad27, and this interaction strongly stimulates the flap endonuclease activity of Rad27 (37). An important question is whether there are additional proteins that contribute to the removal of Okazaki fragment flaps.

The MMR system corrects DNA polymerase errors on newly replicated DNA (38-41). It has been unknown whether the MMR system plays a direct role in DNA replication. In this report, we describe genetic and biochemical experiments that indicate that the MMR system removes 1-nt Okazaki fragment flaps.

EXPERIMENTAL PROCEDURES

Yeast strains and genetic methods

S. cerevisiae wild-type haploid strains used in this study were FKY688 (*MAT*α *ade5-1 lys2::InsE-*A_{14} *trp1-289 his7-2 leu2-3,112 ura3-52 V29617::URA3*) (42), E134 (*MAT*α *ade5-1 lys2::InsE-*A_{14} *trp1-289 his7-2 leu2-3,112 ura3-52*) (43), E35 (*MAT*α *ade5-1 lys2::InsE-*A_8 *trp1-289 his7-2 leu2-3,112 ura3-52)* (43), BY4742 (*MAT*α *his3*Δ*1 leu2*Δ*0 lys2*Δ*0 ura3*Δ*0)*, and 1B-D770 (*MATa ade5-1 lys2::Tn5-13 trp1-289 his7-2 leu2-3,112 ura3-4*) (44). The wild-type diploid strain FKY1037 was prepared by crossing the E134 and 1B-D770 strains. Gene replacements were generated by transforming yeast haploid or diploid cells with disruption cassettes in the presence of lithium acetate/PEG4,000/DMSO. The *PMS1* gene located in its natural chromosomal location was mutated to the *pms1-E707K* allele using the "dellitto perfetto" technique (45). Spontaneous mutation rates were measured and mutation spectra were determined as previously described (42).

Oligonucleotides

Oligonucleotides used in this work were synthesized by IDT (Coralville, IA). The sequences of the indicated oligonucleotides are shown in **Table 1**.

Proteins

Human MutSα, MutLα, MutLα-D699N, MutLα-E705K, MutLα-EA, PCNA, RFC, RPA, CAF-1, histone H3-H4 complex, and FEN1 were isolated in nearly homogenous forms as previously described (23,25,30,46). Yeast MutSα containing the FLAG tag at the N-terminus of its Msh6 subunit was expressed in and purified from insect Sf9 cells. The protein that was used in the DNA-binding reactions was more than 95% pure.

Gel mobility shift assays

Gel mobility shift assays that used the oligonucleotide-based substrates (**Fig. 2**) were carried out as described below. The oligonucleotide-based substrates were produced using oligonucleotides 1-8 (**Table 1**). Each of the substrates contained oligonucleotide 1 which was labeled with ^{32}P at the 5′ end with T4 polynucleotide kinase. In addition, the homoduplex, 1-nt insertion, dynamic 1-nt DNA flap, static 1-nt 3′ DNA flap, static 1-nt 5′ DNA flap, and nicked substrates contained oligonucleotides 2, 3, 4 and 5, 6 and 7, 4 and 8, and 4 and 7, respectively. To make the DNA substrates, the indicated oligonucleotides were mixed and annealed. The annealing was carried out in a buffer containing 20 mM HEPES-NaOH, pH 7.4, and 100 mM KCl at 40°C for 4 h, followed by incubation of the mixtures at 20°C for 30 min. After annealing, the resulting duplex DNAs were separated on native 6% polyacrylamide gels and then purified from the gels. The gel-purified DNAs were used as

substrates in the DNA-binding reactions. The DNA-binding reactions were carried out in 20-µl mixtures each containing 20 mM HEPES-NaOH, pH 7.4, 5 mM $MgCl_2$, 140 mM KCl, 0.2 mg/ml BSA, 2 mM DTT, 20 nM of a competitor 40-bp DNA, 2 nM of the indicated ^{32}P-labeled DNA substrate, and purified yeast or human MutSα. Yeast MutSα concentration in the mixtures varied in the range of 5-1600 nM (the actual concentrations used were 5 nM, 10 nM, 20 nM, 40 nM, 100 nM, 200 nM, 400 nM, 550 nM, 800 nM, 1200 nM, and 1600 nM). Human MutSα concentration in the mixtures was in the range of 5-800 nM (the actual concentrations used were 5 nM, 10 nM, 20 nM, 40 nM, 100 nM, 200 nM, 400 nM, 550 nM, and 800 nM). The competitor 40-bp DNA was prepared by annealing two complementary phosphorylated 40-mer oligonucleotides 9 and 10. Reaction mixtures containing yeast MutSα were incubated for 10 min at 30°C, and reaction mixtures containing human MutSα were incubated for 5 min at 37°C. The reaction products were immediately subjected to electrophoresis on 6% polyacrylamide gels in the 0.5 x Tris-Borate-EDTA running buffer at 4°C. The gels were dried and ^{32}P-labeled DNAs were visualized with a Typhoon phosphorimager (GE HealthCare). Each experiment was repeated at least twice. After quantification of the images with ImageQuant software (GE HealthCare), the apparent K_ds were determined using GraphPad Prism 6 software. The data were fit into the equation of nonlinear regression curve with variable Hill slope ($Y=B_{max}* X^h/(K_d+X^h)$). In this equation, Y is the concentration of MutSα-DNA complexes, B_{max} is the maximum concentration of MutSα-DNA complexes, X is the concentration of MutSα, K_d is the apparent dissociation constant, and h is the Hill coefficient.

Gel mobility shift assays that used 2-kb circular DNA substrates (**Fig. 3**) were performed as detailed below. The substrates were prepared using the pSYAH1A plasmid DNA containing a 36-nt gap (47). The gap was generated according to a described protocol (47). The no-flap, G-T, 1-nt DNA flap, and 1-nt RNA flap substrates were prepared by annealing the gapped pSYAH1A DNA with oligonucleotide 11, 12, 13, and 14, respectively. The G-T and no-flap substrates each contain two ligatable nicks that are 36-nt apart. Cleavage with restriction endonucleases HindIII and HpyCH4III was utilized to determine what fraction of each of the substrates contains the annealed oligonucleotide. These restriction endonucleases do not cleave DNA within a gap due to the destruction of their sites by the gap. Based on this approach, we determined that ~95% of each of the circular substrates contained the annealed oligonucleotide.

To determine apparent K_ds for binding of human MutSα to the circular DNAs, the reactions were carried out in 20-µl mixtures each containing 20-mM HEPES-NaOH, pH 7.4, 120 mM KCl, 5 mM $MgCl_2$, 0.2 mM ATP, 0.2 mg/ml BSA, 2 mM DTT, 1.9 nM (50 ng) of the indicated circular 2-kb DNA, 50 nM of the competitor 40-bp DNA, and human MutSα (5 nM, 10 nM, 20 nM, 40 nM, 100 nM, 200 nM, 400 nM, 550 nM, or 800 nM). After a 5-min incubation at 37°C, each reaction mixture was mixed with 3-µl loading buffer (1xTAE, 40% glycerol, and 0.02% bromophenol blue), and the reaction products were immediately subjected to electrophoresis on 1.2% agarose gels in 1xTAE at 4°C, followed by ethidium bromide staining of the gels. The separated DNAs were transferred onto nylon membranes and hybridized with ^{32}P-labeled oligonucleotide 15. The labeled DNAs were visualized with a Typhoon phosphorimager. The data were quantified and analyzed as described above.

DNA incision reactions

Circular DNAs were used as substrates in the incision reactions (**Fig. 4-8**). Each of the substrates was prepared by annealing of an appropriate 5′-phosphorylated or 5′-^{32}P-labeled oligonucleotide to the gapped pSYAH1A DNA in a mixture containing the oligonucleotide and gapped DNA in a 1:1 molar ratio. The diagnostic cleavage with HindIII and HpyCH4III outlined above showed that 92%-96% of each of the substrates contained the annealed oligonucleotide. The 5′-^{32}P-label was introduced into the oligonucleotides by T4 polynucleotide kinase. The incision reactions were performed in 25-40 µl mixtures each containing 20-mM HEPES-NaOH, pH 7.4, 120 mM KCl, 5 mM $MgCl_2$, 3 mM ATP, 0.2 mg/ml BSA, 2 mM DTT, 1.5 nM (60 fmol) of the indicated DNA substrate, and the indicated human proteins. When MutSα, MutLα, PCNA, RFC, RPA, CAF-1, MutLα-E705K, MutLα-D699N, and MutLα-EA were present in the reaction mixtures, their concentrations were 40 nM, 16 nM, 24 nM, 4 nM, 40 nM, 24 nM, 16 nM, 16 nM, and 16 nM, respectively. Some DNA incision reactions (**Fig. 6-8**) occurred in the presence of histone H3-H4

heterodimer (22 nM, 44 nM, or 88 nM). The DNA incision reactions were incubated at 37°C for 10-30 min as indicated. Unless noted otherwise, the reactions were stopped and analyzed as described below. At the specified times, 8-µl or 11-µl aliquots of the reactions were mixed with 20-µl of a gel-loading buffer containing 90% formamide and 20 mM EDTA. DNA products of the stopped reactions were separated on 15% polyacrylamide gels containing 6 M urea. The gels were dried and the ^{32}P-labeled DNA species were visualized by phosphorimaging. The data were quantified using ImageQuant software (GE HealthCare).

RESULTS

The MMR system and Rad27 flap endonuclease have overlapping functions involved in the maintenance of genome stability

We began this work to investigate whether the MMR system contributes to the removal of Okazaki fragment flaps. The Rad27/FEN1 endonuclease is the key enzyme that removes short flaps during Okazaki fragment maturation (33,34). Accordingly, *S. cerevisiae* strains lacking Rad27 are genetically unstable (31,32,48,49). Previous research has demonstrated that both the MMR system and Rad27 are necessary for the suppression of mutations in the +1 frameshift reporter *his7-2* (32,38-40,44). +1 frameshifts that occur in a 51-bp *his7-2* sequence containing an A_7 run revert the phenotype of the cells to His^+ (42,44). To study whether there is a functional overlap between the MMR system and the Rad27 flap endonuclease, we determined the *his7-2* mutation rates in the haploid and diploid yeast strains shown in **Tables 2-3**. The *his7-2* mutation rate in the haploid double mutant *msh2Δ rad27Δ* ($6{,}700 \times 10^{-8}$) was 33 times higher than the sum of the *his7-2* mutation rates in the haploid single mutants *msh2Δ* and *rad27Δ* (i.e. combining *msh2Δ* with *rad27Δ* resulted in a 33-fold synergistic increase in the *his7-2* mutation rate) (**Table 2**). Likewise, the *his7-2* mutation rate for the diploid double mutant *msh2Δ/msh2Δ rad27Δ/rad27Δ* ($13{,}000 \times 10^{-8}$) was increased 36 times relative to the sum of the *his7-2* mutation rates for the diploid single mutants *msh2Δ/msh2Δ RAD27/RAD27* and *MSH2/MSH2 rad27Δ/rad27Δ* (**Table 3**). These findings indicate that there is a functional overlap between the MMR system and Rad27 in haploid and diploid yeast *S. cerevisiae*.

lys2::InsE-A$_8$ is a yeast +1 frameshift reporter (43). +1 frameshifts that are formed within a 71-bp *lys2::InsE-A$_8$* region including an A_8 run produce Lys^+ cells (43). To ascertain that the above findings (**Tables 2-3**) were not reporter-specific, we measured the *lys2::InsE-A$_8$* mutation rates in the *msh2Δ*, *rad27Δ*, and *msh2Δ rad27Δ* mutants (**Table 4**). Analysis of the data demonstrated that the *lys2::InsE-A$_8$* mutation rate in the *msh2Δ rad27Δ* double mutant ($21{,}000 \times 10^{-8}$) was 24 times higher than the sum of the *lys2::InsE-A$_8$* mutation rates in the *msh2Δ* and *rad27Δ* single mutants. Thus, the use of the *lys2::InsE-A$_8$* mutation assay provided additional evidence that a genetic stabilization function of the MMR system overlaps with a genetic stabilization function of the Rad27 flap endonuclease. Collectively, these genetic experiments suggest that an MMR system-dependent mechanism and a different mechanism dependent on the Rad27 flap endonuclease repair the same or related types of pre-mutagenic intermediates which, if left unrepaired, give rise to +1 frameshifts.

Next, we used DNA sequencing to identify +1 frameshifts that reverted *his7-2* in the *msh2Δ*, *rad27Δ*, and *msh2Δ rad27Δ* mutants (**Table 2**). The results revealed that all of the *his7-2* reversions in the *msh2Δ* and *msh2Δ rad27Δ* spectra and a majority of the reversions in the *rad27Δ* spectrum were 1-bp insertions, each of which extended the A_7 run into an A_8 run (**Table 2**). In addition, we found that combining *msh2Δ* with *rad27Δ* led to a 40-fold synergistic increase in the rate of 1-bp insertions (**Table 2**). This finding implies that one or several related types of pre-mutagenic intermediates producing 1-bp insertions are repaired by both an MMR system-dependent mechanism and a Rad27-dependent mechanism.

The MMR system contains two mismatch recognition complexes, MutSα and MutSβ. As shown in **Table 5,** the *his7-2* mutation rate in the *msh3Δ msh6Δ* mutant was indistinguishable from that in the *msh2Δ* mutant, but 23 times higher than the sum of those in the *msh3Δ* and *msh6Δ* mutants. This result indicates that the partially overlapping activities of MutSα and MutSβ (19,50-52) are engaged in the suppression of +1 frameshifts in *his7-2*. To study whether an MMR system-dependent function overlapping with a Rad27 function involves MutSα and/or MutSβ, we determined the *his7-2* mutation rates for the *msh2Δ*, *rad27Δ*, *msh2Δ rad27Δ*, *msh3Δ msh6Δ rad27Δ*, *msh3Δ rad27Δ*, and *msh6Δ rad27Δ*

mutants (**Table 5**). We found that the *his7-2* mutation rate for the *msh3Δ msh6Δ rad27Δ* mutant did not differ from the *his7-2* mutation rate for the *msh2Δ rad27Δ* mutant, but was ~12 or ~70 times higher than the rate for the *msh6Δ rad27Δ* or *msh3Δ rad27Δ* mutants, respectively. These data indicate that both MutSα and MutSβ participate in an MMR system-dependent function that overlaps with a Rad27 function. We also found that the *his7-2* mutation rate in *msh6Δ rad27Δ* exceeded that in *msh3Δ rad27Δ* by six fold (**Table 5**). This result is consistent with the view that compared to MutSβ, MutSα plays a more important role in an MMR system-dependent function that overlaps with a Rad27 function.

MutLα endonuclease is a key component of the eukaryotic MMR system (9,13,14,25,26,38,39). The endonuclease activity of yMutLα depends on the integrity of the Pms1 DQHA$(X)_2$E$(X)_4$E motif, which is part of the putative active site of the endonuclease (25,26,53,54). The E707K substitution, which replaces the first glutamate residue in the DQHA$(X)_2$E$(X)_4$E motif of yMutLα, inactivates the yeast MMR system (26). We found that combining *rad27Δ* with *mlh1Δ, pms1Δ*, or *pms1-E707K* resulted in a 20-26 times synergistic increase in the *his7-2* mutation rate (**Table 5**). Nevertheless, the *his7-2* mutation rate in the *pms1-E707K rad27Δ*, *pms1Δ rad27Δ*, or *mlh1Δ rad27Δ* strain was half that in the *msh2Δ rad27Δ* strain (**Table 5**). Taken together, these data suggest that an MMR system-dependent function overlapping with a Rad27 function often involves the endonuclease activity of MutLα.

The results described above were obtained using the *his7-2* and *lys2::InsE-A$_8$* reversion assays that only allow scoring of +1 frameshifts. Unlike the *his7-2* and *lys2::InsE-A$_8$* reversion assays, the *CAN1* forward mutation assay allows scoring of many different types of genetic alterations including 1-bp insertions, base substitutions, and 1-bp deletions. The *CAN1* forward mutation assay takes advantage of the fact that mutational inactivation of *CAN1* gene encoding arginine permease makes the yeast cell resistant to canavanine, a structural analogue of arginine. In this assay, Can^r cells are selected on a synthetic media that lacks arginine and contains canavanine. To determine *can1* mutation spectrum in an *msh2Δ rad27Δ* strain, we performed a series of experiments summarized in **Fig. 1**. We started this series of experiments by measuring the *CAN1* mutation rates in two sets of *msh2Δ*, *rad27Δ*, and *msh2Δ rad27Δ* strains (**Fig. 1A**). One set of the strains was prepared on the wild-type strain E134 background and the other on the wild-type strain BY4742 background. We chose to measure *CAN1* mutation rates in two sets of yeast strains to exclude the possibility that the data are strain-specific. The results demonstrated that the relative *CAN1* mutation rate in either *msh2Δ rad27Δ* mutant was ~2-times higher than the sum of the relative *CAN1* mutation rates in the isogenic single mutants (i.e., the relative *CAN1* mutation rates in the isogenic *msh2Δ* and *rad27Δ* mutants are in a weak synergistic relationship) (**Fig. 1A**). Similar results were obtained in two earlier studies (48,49). We next determined the *can1* mutation spectra in the wild-type, *msh2Δ*, *rad27Δ*, and *msh2Δ rad27Δ* mutants (**Fig. 1B**). The rates of base substitutions and 1-nt deletions in the *msh2Δ rad27Δ* mutant did not differ significantly from those in the *msh2Δ* mutant. On the other hand, the rate of 1-nt insertions in the *msh2Δ rad27Δ* mutant was 12 times higher than sum of those in the *msh2Δ* and *rad27Δ* mutants. This information supports the view that one or several related types of pre-mutagenic intermediates causing 1-nt insertions are removed by both an MMR-dependent mechanism and a Rad27-dependent mechanism.

Duplications are formed at a high rate in *rad27Δ* mutants (31,32). These duplications have been suggested to be the products of unprocessed Okazaki fragment flaps (31,49). Strikingly, 6-14-bp duplications were produced at a rate of 630×10^{-8} in *CAN1* in the *msh2Δ rad27Δ* strain, but were absent in the *can1* spectra of the *rad27Δ* and *msh2Δ* mutants (**Fig. 1B**). These data suggest that one or several related types of pre-mutagenic intermediates triggering 6-14-bp duplications are removed by both an MMR-dependent mechanism and a Rad27-dependent mechanism.

The Dna2 helicase/nuclease is an essential enzyme that participates in the removal of flaps during Okazaki fragment maturation (33-36). Yeast strains carrying a *dna2* allele, *dna2-1*, are temperature-sensitive (55,56) and show a weak defect in the maintenance of dinucleotide repeats (56). We established that the *his7-2* mutation rate in the *dna2-1* strain was increased 10-fold relative to that in the wild-type strain (**Table 6**). Sequencing of ten independent *HIS7* revertants produced in the *dna2-1* background showed that

nine mutants contained an identical mutation, which was an A insertion in the *his7-2* A_7 run, and one mutant had a deletion of two As in the same run. We then studied the effect of combining *dna2-1* with *msh2Δ* on the *his7-2* mutation rate (**Table 6**). We found that the *his7-2* mutation rate in the *dna2-1 msh2Δ* double mutant was 2-times higher than the sum of those in the single mutants. This observation is consistent with the idea that one or several related types of pre-mutagenic intermediates causing +1 frameshifts are repaired by both an MMR system-dependent mechanism and a Dna2-dependent mechanism.

Recognition of 1-nt DNA flaps by MutSα

We considered two models to explain the observation that combining *msh2Δ* with *rad27Δ* leads to the strong synergistic increases in the rates of spontaneous 1-bp insertions (**Table 2** and **Fig. 1B**). In the first model, DNA polymerase α errors are corrected not only by MMR (57), but also by a Rad27-dependent mechanism, and DNA polymerase α errors that escape both MMR and the Rad27-dependent mechanism produce mutations including 1-bp insertions. However this model is not supported by the observation that the deletion of *RAD27* in the *msh2Δ* strain does not significantly increase the rate of base substitutions (**Fig. 1B**), which are the most common products of DNA polymerase α errors (57,58). Thus, it is unlikely that a considerable fraction of 1-bp insertions formed in *msh2Δ rad27Δ* mutants originate from DNA polymerase α errors. The second model is based on the knowledge that the key function of the 5′ flap endonuclease Rad27 is the removal of short Okazaki fragment flaps (33,34). In this model, 1-nt Okazaki fragment flaps are removed by both a Rad27-dependent mechanism and an MMR system-dependent mechanism, and the unprocessed flaps are converted by misalignment and ligation into 1-bp insertions. Thus, this model suggests that the majority of 1-bp insertions produced in *msh2Δ rad27Δ* mutants are formed from 1-nt Okazaki fragment flaps. Since Okazaki fragment flaps do not cause base substitutions, the second model is consistent with our genetic data (**Table 2** and **Fig. 1B**).

The second model postulates that the MMR system removes 1-nt Okazaki fragment flaps. To determine whether there is evidence for this, we carried out the biochemical experiments described below. We first examined whether yeast MutSα recognizes 1-nt DNA flaps present on the ^{32}P-labeled oligonucleotide-based substrates (**Fig. 2**). The data revealed that yeast MutSα bound the substrate containing the dynamic 1-nt flap with an apparent K_d of 38 ± 2 nM (**Fig. 2A-B**). The control experiments indicated that yeast MutSα bound the 1-nt insertion-containing DNA, nicked DNA, and homoduplex DNA with apparent K_ds of 25 ± 1 nM, 180 ± 10 nM, and 200 ± 8 nM, respectively (**Fig. 2A-B**). Therefore, these experiments demonstrate that yeast MutSα recognizes the dynamic 1-nt flap nearly as efficiently as the 1-nt insertion. We then investigated whether yeast MutSα recognizes static 1-nt 3′ and 5′ flaps. The experiments showed that yeast MutSα bound the static 1-nt 3′ and 5′ flaps with apparent K_ds of 60 ± 2 nM and 55 ± 3 nM, respectively. Thus, yeast MutSα recognizes the static 1-nt 3′ and 5′ flaps with the same affinity. Surprisingly, yeast MutSα detected the static 1-nt 3′ and 5′ flaps somewhat less efficiently than the dynamic 1-nt flap (**Fig. 2A-B**). Since a dAMP residue forms the flap in the dynamic substrate and a dCMP residue produces the flaps in the static substrates, it is possible that yeast MutSα recognizes a flapped dCMP residue less efficiently than a flapped dAMP residue.

We also studied whether human MutSα recognizes the dynamic 1-nt flap (**Fig. 2C**). Our experiments indicated that human MutSα bound the dynamic 1-nt flap with an apparent K_d of 30 ± 1 nM. An apparent K_d for binding of human MutSα to the 1-nt insertion is 30 ± 6 nM. These K_d values are 7-12 times lower than those for binding of human MutSα to the nicked and homoduplex DNAs (**Fig. 2C**). Thus, human MutSα efficiently recognizes the dynamic 1-nt flap. Collectively, these findings support the view that the ability to recognize 1-nt DNA flaps is conserved in eukaryotic MutSα proteins.

We also analyzed whether human MutSα recognizes a dynamic 1-nt flap present on a circular 2-kb DNA (**Fig. 3**). Each of the substrates contained a 1-nt DNA flap, a 1-nt RNA flap, no flap, or a G-T mispair (**Fig. 3A**). The results revealed that MutSα bound the 1-nt DNA and RNA flap-containing DNAs with K_d values of 119 ± 3 nM and 115 ± 10 nM, respectively (**Fig. 3B**). These K_d values are half that of 254 ± 35 nM for the binding of MutSα to the control no-flap DNA. Thus, MutSα detects that the circular DNA carries

a 1-nt flap, which may be a deoxyribonucleotide or ribonucleotide residue.

MutLα endonuclease-dependent removal of 1-nt flaps

Having shown that MutSα recognizes the 1-nt DNA and RNA flaps on the circular DNA, we carried out and analyzed the reconstituted reactions to determine whether these flaps activate human MutLα endonuclease to incise the discontinuous strand in the presence of human MutSα, PCNA, RFC, and RPA (**Fig. 4**). The circular DNAs were used as substrates in these reactions because loaded PCNA, required for the activation of MutLα endonuclease (25-27), slides off of linear DNA. The reactions were performed under conditions that were very similar to those used for the identification of the MutSα-, PCNA-, RFC-, mismatch-, and ATP-dependent endonuclease activity of human MutLα (25). Analysis of the reactions (**Fig. 4A-B**) led to the following observations. First, 34 ± 5% of the discontinuous strand of the 1-nt DNA flap-containing substrate was incised by MutLα, whereas the endonuclease cleaved only 10 ± 2% of the discontinuous strand of the control flap-free substrate. Second, MutLα incised 30 ± 1% of the discontinuous strand of the 1-nt RNA flap. Third, an endonuclease-deficient MutLα variant, MutLα-E705K (25), did not incise the discontinuous strands of the tested substrates. Together, these observations indicate that 1-nt flaps activate MutLα endonuclease to incise the discontinuous strand in the presence of MutSα, PCNA, RFC, and RPA.

To determine whether incision of the discontinuous strand by MutLα results in the removal of flaps, we performed experiments summarized in **Fig. 5**. As shown in lane 2 of **Fig. 5A**, the incubation of MutLα, MutSα, PCNA, RFC, and RPA with the 1-nt DNA flap-containing circular substrate led to incision of the ^{32}P-labeled 37-nt fragment at several sites. The most abundant product of the incision reaction had an apparent length of 5 nt, indicating that the incision occurred at a site that is four nucleotides 3′ to the flap. The incision products were not formed when MutSα, MutLα, RFC, or PCNA was omitted from the reaction mixture, but the omission of RPA did not have a significant effect on the incision (**Fig. 5A,** lanes 3, 4, 6 and 7, and **Fig.5B**). These results indicate that MutSα, MutLα, RFC, and PCNA are required for the incision, but RPA is not. The time-course experiments demonstrated that the incision reaction produced the 5-nt fragment in a time-dependent manner (**Fig. 5C**). The efficiency of the incision of the site located 4 nt downstream from a 1-nt flap was three times higher than that of the same site on the control flap-free substrate (**Fig. 5A**, lanes 2 and 10, and **Fig.5B-C**). Thus, the flap dependence of the MutLα incision was three-fold. Changing the incubation temperature from 37°C to 25°C decreased the flap dependence of the MutLα incision from three- to two-fold (data not shown). MutLα, MutSα, PCNA, and RFC were also required for the incision of the 1-nt RNA flap-containing substrate (**Fig. 5A,** lanes 18-20,22, and 23, and **Fig.5B**). Consistent with previous study (59), the 5-nt incision product containing the 5′ ribonucleotide residue migrated in the gel slightly slower than the 5-nt incision product lacking a ribonucleotide residue (**Fig. 5A,** lanes 2 and 18).

We also studied whether the endonuclease activity of MutLα is necessary for the incision of the discontinuous strand at a 1-nt flap (**Fig. 5A-B**). The replacement of the wild-type MutLα with the endonuclease-deficient MutLα-E705K led to the disappearance of the incision products indicating that the endonuclease activity of MutLα is responsible for the incisions (**Fig. 5A,** lanes 5 and 21, and **Fig. 5B**). Further analysis revealed that the presence of a 1-nt flap did not activate MutLα endonuclease to incise the discontinuous strand immediately upstream from the flap (data not shown). Taken together, these experiments demonstrate that MutSα, RFC, and PCNA activate MutLα endonuclease to incise the discontinuous strand 4 nt downstream from a 1-nt DNA or RNA flap. Since the incision is so close to the flaps, it triggers their dissociation from the substrates.

Newly replicated DNA is rapidly assembled into nucleosomes by a mechanism that depends on the histone H3-H4 chaperone CAF-1 (60-62). The first step in CAF-1-dependent nucleosome assembly is the deposition of histone H3-H4 tetramers. CAF-1-dependent nucleosome assembly probably impacts many processes that take place on the nascent DNA. Consistent with this idea, CAF-1-dependent nucleosome assembly modulates MMR (46,63). Because the MMR system-dependent flap removal (**Fig. 5**) is likely to occur during CAF-1-dependent nucleosome assembly, we studied whether histone H3-H4 deposition by CAF-1 affects the flap-removing

activity of the MMR system. We determined that CAF-1-dependent histone H3-H4 deposition stimulated the flap-removing activity of the MMR system by two-fold (**Fig. 6A**, lanes 11 and 12, and **Fig. 6B**) and increased the flap dependence of the incision from three- to six-fold (**Fig. 6C**). The efficiency of the flap removal was not changed when MutSα and MutLα were added to the reaction mixtures that were incubated with CAF-1, the histone H3-H4 complex, PCNA, RFC, and RPA for 15 min suggesting that the MMR system efficiently removes 1-nt DNA flaps in the presence of pre-loaded H3-H4 tetramers (data not shown). The omission of CAF-1 significantly decreased both the efficiency and flap dependence of the incision (**Fig. 6C**). Control experiments revealed that the flap removal occurring in the presence of CAF-1-dependent histone H3-H4 deposition required both MutSα and MutLα (**Fig. 6A-B**). An endonuclease-deficient MutLα variant, MutLα-D699N (25), as well as a MutLα ATPase mutant, MutLα-EA (64), could not substitute for the wild-type MutLα in the incision reaction. Thus, these experiments demonstrate that the CAF-1-dependent histone H3-H4 deposition promotes the removal of 1-nt DNA flaps by the activated MutLα endonuclease.

We then studied how CAF-1 and the histone H3-H4 complex affect the incision of the discontinuous strand at sites that are distant from the 1-nt flap (**Fig. 7**). Strikingly, the presence of CAF-1 and the histone H3-H4 complex suppressed the MutLα endonuclease-dependent incision of the discontinuous strand at the remote sites (**Fig. 7A**, lanes 9 and 14-16, and **Fig. 7B**). A similar suppression of the MutLα endonuclease-dependent incision of the discontinuous strand was observed in the 6 protein-system containing the histone H3-H4 complex, but not CAF-1 (**Fig. 7A**, lanes 9-12, and **Fig. 7B**). These findings imply that both CAF-1-dependent histone H3-H4 deposition onto the DNA and non-specific binding of the histone H3-H4 complex to the DNA protect the remote sites from the incision by the activated MutLα endonuclease.

Next, we performed experiments to study whether the reconstituted MMR system is able to remove flaps in the presence of FEN1 (**Fig. 8**). The data showed that increasing FEN1 concentration decreased the yield of the product of MutLα endonuclease-dependent flap removal and increased the yield of the product of FEN1-dependent flap removal (**Fig. 8A-C**). In addition, the data indicated that one or several proteins present in the eight-protein system suppressed the flap endonuclease activity of FEN1 (**Fig. 8A**, lanes 3-10, and **Fig. 8C**). These experiments provide evidence that the MMR system removes flaps in the presence of FEN1 and suggest that the flap endonuclease activities of FEN1 and the MMR system compete with each other.

DISCUSSION

High-fidelity DNA replication is required for the maintenance of genome integrity and the suppression of human diseases (65). The MMR system improves the fidelity of DNA replication by correcting the errors of DNA polymerization (3,4,7). We have used genetic analysis and reconstituted systems to study whether the MMR system contributes to the removal of Okazaki fragment flaps. The major findings described in this report are (1) combining *rad27Δ* with *msh2Δ* produces strong synergistic increases in the rates of 1-bp insertions in *his7-2* and *CAN1* (**Table 2** and **Fig. 1B**); (2) combining *rad27Δ* with *mlh1Δ*, *pms1Δ*, or *pms1-E707K* causes a 20-26 times synergistic increase in the rate of +1 frameshifts in *his7-2* (**Table 5**); (3) purified yeast and human MutSα proteins recognize 1-nt flaps (**Fig. 2** and **3**); (4) MutLα endonuclease activated by MutSα, RFC, and PCNA removes 1-nt flaps (**Fig. 5**); (5) the flap-removing activity of the reconstituted MMR system is stimulated by CAF-1-dependent histone H3-H4 deposition (**Fig. 6**); and (6) the reconstituted MMR system removes 1-nt flaps in the presence of FEN1 (**Fig. 8**).

These findings indicate that the eukaryotic MMR system removes a subset of 1-nt Okazaki fragment flaps and support a model illustrated in **Fig. 9**. This model suggests that MutSα, MutLα, PCNA, and RFC provide the minimal set of activities required for the removal of 1-nt Okazaki fragment flaps by the MMR system. According to this model, the mechanism of the removal of a 1-nt Okazaki fragment flap by the MMR system can be divided into three key steps: recognition of the flap by MutSα, activation of MutLα endonuclease by MutSα, PCNA, and RFC, and the removal of the flap by the activated MutLα endonuclease. Our genetic results also suggest that there is an Msh2-dependent, MutLα-independent mechanism of removal of 1-nt Okazaki fragment flaps (**Table 5**). In addition, our genetic results are compatible with

another model. In this model, misalignment and ligation converts some 1-nt Okazaki fragment flaps into 1-nt loops, which are then removed by the strand-specific MMR (8,11,19,28,66). However, it has not yet been demonstrated that a replicative DNA ligase is able to convert 1-nt flaps into 1-nt loops in the presence of Rad27/FEN1 and/or the MMR system.

The absolute *his7-2* mutation rate in the *rad27Δ/rad27Δ msh2Δ/msh2Δ* diploid (**Table 3**) is half that of the previously described strong mutator diploid *pol3-01/pol3-01 msh2Δ/msh2Δ* (40). (The *pol3-01* mutation inactivates the proofreading activity of DNA polymerase δ.) This observation reveals that the MMR system is nearly as important for the removal of +1 frameshift intermediates in *rad27Δ* strains as for the repair of +1 frameshift intermediates in *pol3-01* strains. Genetic interactions between the MMR system and Rad27 have been investigated in the past (31,48,49), but none of the previous studies utilized a +1 frameshift assay or determined *can1* mutation spectrum in a strain that lacks an MMR gene and *RAD27*. Nevertheless, Johnson et al. (48) reported that the relative *CAN1* mutation rate in the *msh2Δ* mutant is in a weak synergistic relationship with that in the *rad27Δ* mutant. Thus, the results of the measurements of the relative *CAN1* mutation rates in the *msh2Δ*, *rad27Δ*, and *msh2Δ rad27Δ* mutants obtained in this work (**Fig. 1A**) and the study of Johnson et al. (48) are consistent with each other.

MutSα was initially identified as an MMR factor that detects single base-base mismatches (11,12). Subsequent work established that MutSα recognizes 1-12 nt insertion/deletion loops (15,19) and damaged base pairs (67). We have described in this report that MutSα recognizes 1-nt DNA/RNA flaps (**Fig. 2-3**). This finding extends the range of potentially mutagenic DNA structures recognized by MutSα. Our genetic experiments support the idea that MutSβ plays a role in the MMR system-dependent removal of 1-nt Okazaki fragment flaps (**Table 5**). Thus, it is possible that MutSβ, like MutSα, recognizes 1-nt DNA/RNA flaps and activates MutLα endonuclease to remove them. This would be in line with previous work that identified that MutSβ specifically binds a variety of DNA recombination structures including the non-complementary 5′ DNA flaps and 3′ tails (68).

In the crystal structure of MutSα-G-T DNA complex, the E434 residue of the conserved mismatch recognition F-X-E motif forms a hydrogen bond with the mispaired T, the conserved F432 residue stacks onto the T, DNA is sharply bent at the mismatch, and there are several non-specific protein-DNA interactions (69). These features are also present in the structures of the prokaryotic MutS-mismatch-containing DNA complexes (70,71). It has been proposed that during mismatch recognition, MutS stacks the conserved F on an unpaired nucleotide residue and bends DNA (70). The intrinsic bendability of duplex DNA at a mismatch is thought to strongly contribute to the recognition of the mismatch by MutS. A recent work has shown that the same mechanism of mismatch recognition is employed by MutSα (69). We speculate that the MSH6 F-X-E motif is responsible for the recognition of flaps by MutSα. If this is the case, the conserved E434 is a strong candidate to interact with a flapped deoxy- or ribonucleotide residue via a hydrogen bond. It has been described that duplex DNA bends at nicks (72). Therefore, DNA bending at a nick that accompanies the flap may facilitate the flap recognition by MutSα. Since the MMR system is conserved from bacteria to humans (69-71), it is possible that the MMR system also contributes to the removal of Okazaki fragment flaps in bacteria.

Eukaryotic DNA transactions occur in the nucleosomal environment. The fact that the size of naked nascent DNA strands at a eukaryotic replication fork is only ~450 bp (73) is consistent with the view that the newly replicated DNA is rapidly assembled into nucleosomes by the histone chaperone CAF-1 (60). Our analysis demonstrates that the CAF-1-dependent histone H3-H4 deposition increases the efficiency and specificity of the flap removal by MutLα and protects the discontinuous strand from MutLα incision at the remote sites (**Fig. 6** and **7**). The mechanism behind these effects is not known. We speculate that the loaded histones H3-H4 tetramers trap the MutLα-containing incision complex at the flap-containing site where it was assembled, and as a result the MutLα is not able to incise the discontinuous strand at the remote sites and instead removes the flap.

Previous research demonstrated that during eukaryotic Okazaki fragment maturation, the strand displacement activity of DNA polymerase δ (30,33,74) produces flaps that are removed by the

Rad27/FEN1 endonuclease (33,34), the 3′-5′ exonuclease activity of DNA polymerase δ (32), and the nuclease/helicase Dna2 (36). In this report, we have described evidence that the eukaryotic MMR system contributes to the removal of Okazaki fragment flaps.

ACKNOWLEDGEMENTS

We are grateful to Paul Modrich for his advice and insightful discussions, Farid F. Kadyrov for critical reading of the manuscript, Francesca Storici and Kirill Lobachev for help with the "dellitto perfetto" technique. We thank Tim Formosa for supplying a *dna2-1* strain and Paul Modrich and Mike Resnick for providing plasmids used in this work.

CONFLICT OF INTEREST

The authors declare that they have no conflicts of interest with the contents of this article.

AUTHOR CONTRIBUTIONS

FK and LK designed experiments. LK, BD, and FK performed experiments and analyzed data. FK and LK wrote the paper.

REFERENCES

1. Modrich, P. (1995) Mismatch repair, genetic stability and tumour avoidance. *Philos. Trans. R. Soc. Lond. B Biol. Sci.* **347**, 89-95

2. Harfe, B. D., and Jinks-Robertson, S. (2000) DNA Mismatch Repair and Genetic Instability. *Annu. Rev. Genet.* **34**, 359-399

3. Kunkel, T. A., and Erie, D. A. (2005) DNA Mismatch Repair. *Annu. Rev. Biochem.* **74**, 681-710

4. Li, G. M. (2008) Mechanisms and functions of DNA mismatch repair. *Cell Res.* **18**, 85-98

5. Jiricny, J. (2013) Postreplicative mismatch repair. *Cold Spring Harb. Perspect. Biol.* **5**, a012633

6. Lynch, H. T., Snyder, C. L., Shaw, T. G., Heinen, C. D., and Hitchins, M. P. (2015) Milestones of Lynch syndrome: 1895-2015. *Nat. Rev. Cancer* **15**, 181-194

7. Iyer, R. R., Pluciennik, A., Burdett, V., and Modrich, P. L. (2006) DNA mismatch repair: functions and mechanisms. *Chem. Rev.* **106**, 302-323

8. Modrich, P. (2006) Mechanisms in eukaryotic mismatch repair. *J. Biol. Chem.* **281**, 30305-30309

9. Strand, M., Prolla, T. A., Liskay, R. M., and Petes, T. D. (1993) Destabilization of tracts of simple repetitive DNA in yeast by mutations affecting DNA mismatch repair. *Nature* **365**, 274-276

10. de Wind, N., Dekker, M., Berns, A., Radman, M., and te Riele, H. (1995) Inactivation of the mouse Msh2 gene results in mismatch repair deficiency, methylation tolerance, hyperrecombination, and predisposition to cancer. *Cell* **82**, 321-330

11. Drummond, J. T., Li, G.-M., Longley, M. J., and Modrich, P. (1995) Isolation of an hMSH2•p160 heterodimer that restores mismatch repair to tumor cells. *Science* **268**, 1909-1912

12. Palombo, F., Gallinari, P., Iaccarino, I., Lettieri, T., Hughes, M., D'Arrigo, A., Truong, O., Hsuan, J. J., and Jiricny, J. (1995) GTBP, a 160-kilodalton protein essential for mismatch-binding activity in human cells. *Science* **268**, 1912-1914

13. Li, G.-M., and Modrich, P. (1995) Restoration of mismatch repair to nuclear extracts of H6 colorectal tumor cells by a heterodimer of human MutL homologs. *Proc. Natl. Acad. Sci. U. S. A.* **92**, 1950-1954

14. Edelmann, W., Cohen, P. E., Kane, M., Lau, K., Morrow, B., Bennett, S., Umar, A., Kunkel, T., Cattoretti, G., Chaganti, R., Pollard, J. W., Kolodner, R. D., and Kucherlapati, R. (1996) Meiotic pachytene arrest in MLH1-deficient mice. *Cell* **85**, 1125-1134

15. Palombo, F., Iaccarino, I., Nakajima, E., Ikejima, M., Shimada, T., and Jiricny, J. (1996) hMutSβ, a heterodimer of hMSH2 and hMSH3, binds to insertion/deletion loops in DNA. *Curr. Biol.* **6**, 1181-1184

16. Johnson, R. E., Kovvali, G. K., Guzder, S. N., Amin, N. S., Holm, C., Habraken, Y., Sung, P., Prakash, L., and Prakash, S. (1996) Evidence for involvement of yeast proliferating cell nuclear antigen in DNA mismatch repair. *J. Biol. Chem.* **271**, 27987-27990

17. Umar, A., Buermeyer, A. B., Simon, J. A., Thomas, D. C., Clark, A. B., Liskay, R. M., and Kunkel, T. A. (1996) Requirement for PCNA in DNA mismatch repair at a step preceding DNA resynthesis. *Cell* **87**, 65-73

18. Tishkoff, D. X., Boerger, A. L., Bertrand, P., Filosi, N., Gaida, G. M., Kane, M. F., and Kolodner, R. D. (1997) Identification and characterization of Saccharomyces cerevisiae EXO1, a gene encoding an exonuclease that interacts with MSH2. *Proc. Natl. Acad. Sci. U. S. A.* **94**, 7487-7492

19. Genschel, J., Littman, S. J., Drummond, J. T., and Modrich, P. (1998) Isolation of hMutSβ from human cells and comparison of the mismatch repair specificities of hMutSβ and hMutSα. *J. Biol. Chem.* **273**, 19895-19901

20. de Wind, N., Dekker, M., Claij, N., Jansen, L., van Klink, Y., Radman, M., Riggins, G., van der Valk, M., van't Wout, K., and te Riele, H. (1999) HNPCC-like cancer predisposition in mice through simultaneous loss of Msh3 and Msh6 mismatch-repair protein functions. *Nat. Genet.* **23**, 359-362

21. Genschel, J., Bazemore, L. R., and Modrich, P. (2002) Human exonuclease I is required for 5' and 3' mismatch repair. *J. Biol. Chem.* **277**, 13302-13311

22. Wei, K., Clark, A. B., Wong, E., Kane, M. F., Mazur, D. J., Parris, T., Kolas, N. K., Russell, R., Hou, H., Jr., Kneitz, B., Yang, G., Kunkel, T. A., Kolodner, R. D., Cohen, P. E., and Edelmann, W. (2003) Inactivation of Exonuclease 1 in mice results in DNA mismatch repair defects, increased cancer susceptibility, and male and female sterility. *Genes Dev.* **17**, 603-614

23. Dzantiev, L., Constantin, N., Genschel, J., Iyer, R. R., Burgers, P. M., and Modrich, P. (2004) A defined human system that supports bidirectional mismatch-provoked excision. *Mol. Cell* **15**, 31-41

24. Pavlov, Y. I., Mian, I. M., and Kunkel, T. A. (2003) Evidence for preferential mismatch repair of lagging strand DNA replication errors in yeast. *Curr. Biol.* **13**, 744-748

25. Kadyrov, F. A., Dzantiev, L., Constantin, N., and Modrich, P. (2006) Endonucleolytic function of MutLalpha in human mismatch repair. *Cell* **126**, 297-308

26. Kadyrov, F. A., Holmes, S. F., Arana, M. E., Lukianova, O. A., O'Donnell, M., Kunkel, T. A., and Modrich, P. (2007) Saccharomyces cerevisiae MutLalpha is a mismatch repair endonuclease. *J. Biol. Chem.* **282**, 37181-37190

27. Pluciennik, A., Dzantiev, L., Iyer, R. R., Constantin, N., Kadyrov, F. A., and Modrich, P. (2010) PCNA function in the activation and strand direction of MutLalpha endonuclease in mismatch repair. *Proc. Natl. Acad. Sci. US A* **107**, 16066-16071

28. Iyer, R. R., Pluciennik, A., Genschel, J., Tsai, M. S., Beese, L. S., and Modrich, P. (2010) MutLalpha and proliferating cell nuclear antigen share binding sites on MutSbeta. *J. Biol. Chem.* **285**, 11730-11739

29. Constantin, N., Dzantiev, L., Kadyrov, F. A., and Modrich, P. (2005) Human mismatch repair: Reconstitution of a nick-directed bidirectional reaction. *J. Biol. Chem.* **280**, 39752-39761

30. Kadyrov, F. A., Genschel, J., Fang, Y., Penland, E., Edelmann, W., and Modrich, P. (2009) A possible mechanism for exonuclease 1-independent eukaryotic mismatch repair. *Proc. Natl. Acad. Sci. USA* **106**, 8495-8500

31. Tishkoff, D. X., Filosi, N., Gaida, G. M., and Kolodner, R. D. (1997) A novel mutation avoidance mechanism dependent on *S. cerevisiae RAD27* is distinct from DNA mismatch repair. *Cell* **88**, 253-263

32. Jin, Y. H., Obert, R., Burgers, P. M., Kunkel, T. A., Resnick, M. A., and Gordenin, D. A. (2001) The 3'-->5' exonuclease of DNA polymerase delta can substitute for the 5' flap endonuclease Rad27/Fen1 in processing Okazaki fragments and preventing genome instability. *Proc. Natl. Acad. Sci. U S A* **98**, 5122-5127

33. Burgers, P. M. (2009) Polymerase dynamics at the eukaryotic DNA replication fork. *J. Biol. Chem.* **284**, 4041-4045

34. Balakrishnan, L., and Bambara, R. A. (2011) Eukaryotic lagging strand DNA replication employs a multi-pathway mechanism that protects genome integrity. *J. Biol. Chem.* **286**, 6865-6870

35. Budd, M. E., and Campbell, J. L. (1995) A yeast gene required for DNA replication encodes a protein with homology to DNA helicases. *Proc. Natl. Acad. Sci. U .S .A.* **92**, 7642-7646

36. Ayyagari, R., Gomes, X. V., Gordenin, D. A., and Burgers, P. M. (2003) Okazaki fragment maturation in yeast. I. Distribution of functions between FEN1 AND DNA2. *J. Biol. Chem.* **278**, 1618-1625

37. Li, X., Li, J., Harrington, J., Lieber, M. R., and Burgers, P. M. (1995) Lagging strand DNA synthesis at the eukaryotic replication fork involves binding and stimulation of FEN-1 by proliferating cell nuclear antigen. *J. Biol. Chem.* **270**, 22109-22112

38. Morrison, A., Johnson, A. L., Johnston, L. H., and Sugino, A. (1993) Pathway correcting DNA replication errors in Saccharomyces cerevisiae. *EMBO J.* **12**, 1467-1473

39. Morrison, A., and Sugino, A. (1994) The 3'-->5' exonucleases of both DNA polymerases delta and epsilon participate in correcting errors of DNA replication in Saccharomyces cerevisiae. *Mol. Gen. Genet.* **242**, 289-296

40. Tran, H. T., Gordenin, D. A., and Resnick, M. A. (1999) The 3'-->5' exonucleases of DNA polymerases delta and epsilon and the 5'-->3' exonuclease Exo1 have major roles in postreplication mutation avoidance in Saccharomyces cerevisiae. *Mol. Cell. Biol.* **19**, 2000-2007

41. Greene, C. N., and Jinks-Robertson, S. (2001) Spontaneous frameshift mutations in Saccharomyces cerevisiae: accumulation during DNA replication and removal by proofreading and mismatch repair activities. *Genetics* **159**, 65-75

42. Kadyrova, L. Y., Mertz, T. M., Zhang, Y., Northam, M. R., Sheng, Z., Lobachev, K. S., Shcherbakova, P. V., and Kadyrov, F. A. (2013) A reversible histone H3 acetylation cooperates with mismatch repair and replicative polymerases in maintaining genome stability. *PLoS Genet.* **9**, e1003899

43. Tran, H. T., Keen, J. D., Kricker, M., Resnick, M. A., and Gordenin, D. A. (1997) Hypermutability of homonucleotide runs in mismatch repair and DNA polymerase proofreading yeast mutants. *Mol. Cell. Biol.* **17**, 2859-2865

44. Shcherbakova, P. V., and Kunkel, T. A. (1999) Mutator phenotypes conferred by MLH1 overexpression and by heterozygosity for mlh1 mutations. *Mol. Cell. Biol.* **19**, 3177-3183

45. Storici, F., Lewis, L. K., and Resnick, M. A. (2001) In vivo site-directed mutagenesis using oligonucleotides. *Nat. Biotechnol.* **19**, 773-776

46. Kadyrova, L. Y., Rodriges Blanko, E., and Kadyrov, F. A. (2011) CAF-I-dependent control of degradation of the discontinuous strands during mismatch repair. *Proc. Natl. Acad. Sci. U S A* **108**, 2753-2758

47. York, S. J., and Modrich, P. (2006) Mismatch repair-dependent iterative excision at irreparable O6-methylguanine lesions in human nuclear extracts. *J. Biol. Chem.* **281**, 22674-22683

48. Johnson, R. E., Kovvali, G. K., Prakash, L., and Prakash, S. (1995) Requirement of the yeast RTH1 5' to 3' exonuclease for the stability of simple repetitive DNA. *Science* **269**, 238-240

49. Xie, Y., Liu, Y., Argueso, J. L., Henricksen, L. A., Kao, H. I., Bambara, R. A., and Alani, E. (2001) Identification of rad27 mutations that confer differential defects in mutation avoidance, repeat tract instability, and flap cleavage. *Mol. Cell. Biol.* **21**, 4889-4899

50. Johnson, R. E., Kovvali, G. K., Prakash, L., and Prakash, S. (1996) Requirement of the yeast MSH3 and MSH6 genes for MSH2-dependent genomic stability. *J. Biol. Chem.* **271**, 7285-7288

51. Marsischky, G. T., Filosi, N., Kane, M. F., and Kolodner, R. (1996) Redundancy of *Saccharomyces cerevisiae* MSH3 and MSH6 in MSH2-dependent mismatch repair. *Genes Dev.* **10**, 407-420

52. Harfe, B. D., and Jinks-Robertson, S. (1999) Removal of frameshift intermediates by mismatch repair proteins in Saccharomyces cerevisiae. *Mol. Cell. Biol.* **19**, 4766-4773

53. Pillon, M. C., Lorenowicz, J. J., Uckelmann, M., Klocko, A. D., Mitchell, R. R., Chung, Y. S., Modrich, P., Walker, G. C., Simmons, L. A., Friedhoff, P., and Guarne, A. (2010) Structure of the endonuclease domain of MutL: unlicensed to cut. *Mol. Cell* **39**, 145-151

54. Gueneau, E., Dherin, C., Legrand, P., Tellier-Lebegue, C., Gilquin, B., Bonnesoeur, P., Londino, F., Quemener, C., Le Du, M. H., Marquez, J. A., Moutiez, M., Gondry, M., Boiteux, S., and Charbonnier, J. B. (2013) Structure of the MutLalpha C-terminal domain reveals how Mlh1 contributes to Pms1 endonuclease site. *Nat. Struct. Mol. Biol.* **20**, 461-468

55. Formosa, T., and Nittis, T. (1999) Dna2 mutants reveal interactions with Dna polymerase alpha and Ctf4, a Pol alpha accessory factor, and show that full Dna2 helicase activity is not essential for growth. *Genetics* **151**, 1459-1470

56. Budd, M. E., and Campbell, J. L. (2000) The pattern of sensitivity of yeast dna2 mutants to DNA damaging agents suggests a role in DSB and postreplication repair pathways. *Mutat. Res.* **459**, 173-186

57. Nick McElhinny, S. A., Kissling, G. E., and Kunkel, T. A. (2010) Differential correction of lagging-strand replication errors made by DNA polymerases {alpha} and {delta}. *Proc. Natl. Acad. Sci. U S A* **107**, 21070-21075

58. Kunkel, T. A. (1985) The mutational specificity of DNA polymerases-alpha and -gamma during in vitro DNA synthesis. *J. Biol. Chem.* **260**, 12866-12874

59. Nick McElhinny, S. A., Watts, B. E., Kumar, D., Watt, D. L., Lundstrom, E. B., Burgers, P. M., Johansson, E., Chabes, A., and Kunkel, T. A. (2010) Abundant ribonucleotide incorporation into DNA by yeast replicative polymerases. *Proc. Natl. Acad. Sci. U S A* **107**, 4949-4954

60. Smith, S., and Stillman, B. (1989) Purification and characterization of CAF-I, a human cell factor required for chromatin assembly during DNA replication in vitro. *Cell* **58**, 15-25

61. Smith, S., and Stillman, B. (1991) Stepwise assembly of chromatin during DNA replication in vitro. *EMBO J* **10**, 971-980

62. Kadyrova, L. Y., Rodriges Blanko, E., and Kadyrov, F. A. (2013) Human CAF-1-dependent nucleosome assembly in a defined system. *Cell Cycle* **12**, 3286-3297

63. Schopf, B., Bregenhorn, S., Quivy, J. P., Kadyrov, F. A., Almouzni, G., and Jiricny, J. (2012) Interplay between mismatch repair and chromatin assembly. *Proc .Natl. Acad. Sci. U S A* **109**, 1895-1900

64. Raschle, M., Dufner, P., Marra, G., and Jiricny, J. (2002) Mutations within the hMLH1 and hPMS2 subunits of the human MutLalpha mismatch repair factor affect its ATPase activity, but not its ability to interact with hMutSalpha. *J. Biol. Chem.* **277**, 21810-21820

65. Kunkel, T. A. (2004) DNA replication fidelity. *J. Biol. Chem.* **279**, 16895-16898

66. Pena-Diaz, J., and Jiricny, J. (2012) Mammalian mismatch repair: error-free or error-prone? *Trends Biochem. Sci.* **37**, 206-214

67. Duckett, D. R., Drummond, J. T., Murchie, A. I. H., Reardon, J. T., Sancar, A., Lilley, D. M. J., and Modrich, P. (1996) Human MutSα recognizes damaged DNA base pairs containing O^6-methylguanine, O^4-methylthymine or the cisplatin-d(GpG) adduct. *Proc. Natl. Acad. Sci. U. S. A.* **93**, 6443-6447

68. Surtees, J. A., and Alani, E. (2006) Mismatch repair factor MSH2-MSH3 binds and alters the conformation of branched DNA structures predicted to form during genetic recombination. *J. Mol. Biol.* **360**, 523-536

69. Warren, J. J., Pohlhaus, T. J., Changela, A., Iyer, R. R., Modrich, P. L., and Beese, L. S. (2007) Structure of the human MutSalpha DNA lesion recognition complex. *Mol. Cell* **26**, 579-592

70. Lamers, M. H., Perrakis, A., Enzlin, J. H., Winterwerp, H. H., de Wind, N., and Sixma, T. K. (2000) The crystal structure of DNA mismatch repair protein MutS binding to a G-T mismatch. *Nature* **407**, 711-717

71. Obmolova, G., Ban, C., Hsieh, P., and Yang, W. (2000) Crystal structures of mismatch repair protein MutS and its complex with a substrate DNA. *Nature* **407**, 703-710

72. Kuhn, H., Protozanova, E., and Demidov, V. V. (2002) Monitoring of single nicks in duplex DNA by gel electrophoretic mobility-shift assay. *Electrophoresis* **23**, 2384-2387

73. Lucchini, R., Wellinger, R. E., and Sogo, J. M. (2001) Nucleosome positioning at the replication fork. *EMBO J.* **20**, 7294-7302

74. Garg, P., Stith, C. M., Sabouri, N., Johansson, E., and Burgers, P. M. (2004) Idling by DNA polymerase delta maintains a ligatable nick during lagging-strand DNA replication. *Genes Dev.* **18**, 2764-2773

FOOTNOTES

Research reported in this publication was supported by the National Institute of General Medical Sciences of the National Institutes of Health under Award Number R01GM095758. The content is solely the responsibility of the authors and does not necessarily represent the official views of the National Institutes of Health.

FIGURE LEGENDS

Figure 1. *CAN1* mutation rates and *can1* mutation spectra in the wild-type, *msh2Δ*, *rad27Δ*, and *msh2Δ rad27Δ* strains. (**A**) *CAN1* mutation rates. Each of the mutants was made in the two different wild-type backgrounds: E134 and BY4742. The numbers above the bars are the relative mutation rates. (**B**) *can1* mutation spectra in the wild-type strain E134 and its mutant derivatives. The relative mutation rates are in parentheses. [a], all 1-bp insertions were formed in mononucleotide runs that were ≥2N.

Figure 2. Human and yeast MutSα proteins recognize 1-nt DNA flaps. The gel mobility shift assays with the oligonucleotide-based DNA substrates and calculations of the apparent K_ds were performed as described in "EXPERIMENTAL PROCEDURES". All six substrates had the same bottom strand. The DNA sequences of the homoduplex and nicked DNA substrates were identical to each other and to the *his7-2* sequence, in which the majority of +1 frameshifts are formed. Compared to the top strand of the homoduplex or nicked substrate, the top strands of the flapped and 1-nt insertion substrates each contained an extra nucleotide residue, which was necessary to produce the 1-nt flap or 1-nt insertion. (**A**) Representative images showing binding of yeast MutSα to the different DNA substrates. Each DNA-binding reaction was carried out in the mixture containing the indicated concentration of yeast MutSα and the indicated DNA substrate (2 nM). (**B**) and (**C**) Apparent K_ds for binding of yeast MutSα (**B**) and human MutSα (**C**) to the indicated DNA substrates. The apparent K_ds were calculated using the data that were obtained by quantification of images including those shown in (**A**). The numbers above the bars are the apparent K_ds.

Figure 3. Human MutSα recognizes 1-nt DNA and RNA flaps on 2-kb circular DNA molecules. (**A**) Diagrams of the 2-kb circular DNAs used in the DNA-binding reactions. Each diagram also shows the relative position of the hybridization probe (a bar with an asterisk). The hybridization probe is complementary to the continuous strand. (**B**) Apparent K_ds for binding of human MutSα to the indicated circular substrates. The numbers above the bars are the apparent K_ds. The gel mobility shift assays and calculations of the apparent K_ds were carried out as detailed in "EXPERIMENTAL PROCEDURES".

Figure 4. 1-nt DNA and RNA flaps activate MutLα endonuclease to incise the discontinuous strands in the presence of MutSα, PCNA, RFC, and RPA. Each DNA incision reaction was carried out in the mixture containing the indicated human proteins and DNA substrate (1.5 nM). When MutSα, MutLα, MutLα-E705K, PCNA, RFC, and RPA were present in the reaction mixtures, their concentrations were 40 nM, 16 nM, 16 nM, 24 nM, 4 nM, and 40 nM, respectively. After a 10-min incubation, the reactions were stopped by the addition of NaOH and EDTA to the final concentrations of 40 mM and 5 mM, respectively. The reaction products were separated on alkaline 1.2% agarose gels, transferred onto nylon membranes, hybridized with ^{32}P-labeled oligonucleotide 16, and visualized by phosphorimaging. (**A**) Representative images showing incision of the discontinuous strands in the presence of MutLα, MutSα, PCNA, RFC, and RPA. The diagrams outline the circular DNA substrates. Each diagram also shows the relative position of the hybridization probe (a bar with an asterisk). The hybridization probe is complementary to the discontinuous strand. (**B**) Summary of incision of the discontinuous strands of the indicated DNA substrates at sites that are 4-nt 3′ to the flap or control nick. The data were obtained by quantification of images including those shown in (**A**) and are presented as averages ± 1 SD, n≥3.

Figure 5. MutLα endonuclease incises the discontinuous strand four nucleotides downstream from a 1-nt DNA or RNA flap. The 37-nt fragments of the 1-nt DNA and RNA flap-containing substrates and the 36-nt fragments of the control flap-free and G-T substrates were labeled at their 5′ ends with ^{32}P. Each DNA incision reaction was performed in the mixture containing the indicated human proteins and ^{32}P-labeled DNA substrate (1.5 nM). When MutSα, MutLα, MutLα-E705K, PCNA, RFC, and RPA were present in the reaction mixtures, their concentrations were 40 nM, 16 nM, 16 nM, 24 nM, 4 nM, and 40 nM, respectively. The DNA incision reactions were stopped and analyzed as described in "EXPERIMENTAL PROCEDURES". (**A**) Representative image showing MutLα endonuclease-

dependent incision of the discontinuous strand 4 nt downstream from the 1-nt flap. The incision reactions were incubated for 10 min. The diagrams outline the circular DNA substrates. (**B**) Summary of incision of the discontinuous strands of the indicated substrates at sites that are 4-nt 3′ to the flap or control nick. The DNA incision reactions were incubated for 10 min. (**C**) Time course of incision of the discontinuous strands of the indicated substrates at sites that are 4-nt 3′ to the flap or control nick. The incision reactions were carried out in the mixtures containing MutSα (40 nM), MutLα (16 nM), PCNA (24 nM), RFC (4 nM), RPA (40 nM), and the indicated DNA substrate (1.5 nM). The data in (**B**) and (**C**) are averages ± 1 SD ((**B**): n≥4 and (**C**): n≥3) and were obtained by quantification of images including the one shown in (**A**).

Figure 6. CAF-1-dependent histone H3-H4 deposition stimulates the removal of 1-nt flaps by the activated MutLα endonuclease. The 37-nt fragment of the 1-nt DNA flap-containing substrate and the 36-nt fragment of the control flap-free substrate were labeled at their 5′ ends with ^{32}P. Each DNA incision reaction was performed in the mixture containing the indicated human proteins and ^{32}P-labeled DNA substrate (1.5 nM). When MutSα, MutLα, MutLα-D699N, MutLα-EA, PCNA, RFC, RPA, CAF-1, and the histone H3-H4 heterodimer were present in the reaction mixtures, their concentrations were 40 nM, 16 nM, 16 nM, 16 nM, 24 nM, 4 nM, 40 nM, 24 nM, and 88 nM, respectively. The reactions were incubated for 30 min and then stopped and analyzed as described in "EXPERIMENTAL PROCEDURES". (**A**) Representative image showing the effects of the indicated protein combinations on incision of the discontinuous strands of the indicated substrates at sites that are 4-nt 3′ from the flap or control nick. The diagrams outline the circular DNA substrates. (**B**) Graphical representation the effects of the indicated protein combinations on incision of the discontinuous strands of the indicated substrates at sites that are 4-nt 3′ from the flap or control nick. The data were obtained by quantification of images including the one shown in (**A**) and are averages ± 1 SD (n≥4). (**C**) Dependence of the incision on the presence of the 1-nt DNA flap. The flap dependence values were calculated from the data shown in (**B**). The presence of a statistically significant difference between the flap dependences of the two indicated reactions was identified by unpaired t-test.

Figure 7. CAF-1-dependent histone H3-H4 deposition protects the remote sites from incision by MutLα endonuclease. Each DNA incision reaction was performed in the mixture containing the indicated human proteins and DNA substrate (1.5 nM). When MutSα, MutLα, PCNA, RFC, RPA, and CAF-1 were present in the reaction mixtures, their concentrations were 40 nM, 16 nM, 24 nM, 4 nM, 40 nM, and 24 nM, respectively. After a 30-min incubation, the incision reactions were stopped and analyzed as described in **Fig. 4**. (**A**) Image showing the effects of the different protein combinations on incision of the discontinuous strands of the 1-nt flap-containing and flap-free DNA substrates. The diagrams outline the DNA substrates. Each diagram also shows the relative position of the hybridization probe (a bar with an asterisk), which is complementary to the discontinuous strand. (**B**) and (**C**) Incision of the discontinuous strands of the 1-nt flap-containing and flap-free DNA substrates as a function of concentration of histone H3-H4 heterodimers. The data were obtained by quantification of images including the one shown in (**A**) and presented as averages ± 1 SD, n=2.

Figure 8. Flap removal in a reconstituted human system containing FEN1 and MutLα endonucleases. The DNA incision reactions were carried out in the mixtures containing the indicated human proteins and ^{32}P-labeled circular DNA substrate (1.5 nM). When MutSα, MutLα, PCNA, RFC, RPA, CAF-1, and the histone H3-H4 heterodimer were present in the reaction mixtures, their concentrations were 40 nM, 16 nM, 24 nM, 4 nM, 40 nM, 24 nM, and 88 nM, respectively. After incubation for 10 min, the DNA incision reactions were stopped and analyzed as described in "EXPERIMENTAL PROCEDURES". (**A**) Representative image showing the effects of the different protein combinations on the removal of the 1-nt DNA flaps. The arrows indicate the positions of the 1-nt and 5-nt cleavage products generated by FEN1 and MutLα, respectively. The diagram outlines the circular DNA substrate. (**B**) Graphical representation of the effects of the different FEN1 concentrations on the yield of the product of MutLα endonuclease-dependent flap removal in the eight-protein system. The eight-protein system contained MutLα (16 nM), MutSα (40 nM), PCNA (24 nM), RFC (4 nM), RPA

(40 nM), CAF-1 (24 nM), histone H3-H4 heterodimer (88 nM), and FEN1 (0.3 nM, 0.6 nM, 1.2 nM, or 2.4 nM). (**C**) Graphical representation of the effects of the different FEN1 concentrations on the yield of the product of FEN1-dependent flap removal in the one-protein and eight-protein systems. The one-protein system contained FEN1 (0.3 nM, 0.6 nM, 1.2 nM, or 2.4 nM). The data in (**B**) and (**C**) were obtained by quantification of images including the one shown in panel (**A**), and are averages ± 1 SD ($n \geq 4$).

Figure 9. Role for the MMR system in DNA replication. The model suggests that the MMR system supports DNA replication by removing 1-nt Okazaki fragment flaps. The process of the removal of a 1-nt Okazaki fragment flap by the MMR system is initiated by the recognition of the flap by MutSα. In the next step, MutSα acts in conjunction with PCNA and RFC to activate MutLα endonuclease. The activated MutLα endonuclease then removes the flap.

TABLES

Table 1. The sequences of oligonucleotides described in this report

Oligonucleotide	Oligonucleotide sequence
1	5′-AACCGTCATTTTCTAGGTTTTTTTCTTTTCTGAATTCAGAA-3′
2	5′-TTCTGAATTCAGAAAAGAAAAAAACCTAGAAAATGACGGTT-3′
3	5′-TTCTGAATTCAGAAAAGAAAAAAAACCTAGAAAATGACGGTT-3′
4	5′-TTCTGAATTCAGAAAAGAAAA-3′
5	5′-AAAACCTAGAAAATGACGGTT-3′
6	5′-TTCTGAATTCAGAAAAGAAAAC-3′
7	5′-AAACCTAGAAAATGACGGTT-3′
8	5′-CAAACCTAGAAAATGACGGTT-3′
9	5′-CGCCGAATTGCTAGCAAGCTTTCGAGTCTAGAAATTCGGC-3′
10	5′-GCCGAATTTCTAGACTCGAAAGCTTGCTAGCAATTCGGCG-3′
11	5'-GCTACCGTCCTCGAAGCTTCCGCATCGGAGTCGACG-3'
12	5'-GCTACCGTCCTCGAGGCTTCCGCATCGGAGTCGACG-3'
13	5'-CGCTACCGTCCTCGAAGCTTCCGCATCGGAGTCGACG-3'
14	5'-rCGCTACCGTCCTCGAAGCTTCCGCATCGGAGTCGACG-3'
15	5′-GACAGTTACCAATGCTTAATCAGTG-3′
16	5′-GCAGCGAGGCAGTGAGCGAGGAAGC-3′

Oligonucleotides 1-14 were gel-purified by IDT (Coralville, IA).

Table 2. Impact of deletion of *MSH2* and *RAD27* on rates of *his7-2* mutations

Relevant genotype	***his7-2* mutation rate**		**Rates of indicated *his7-2* mutations (x 10^{-8})**		
	Absolute mutation rate (x 10^{-8})	**Relative rate**	**1-bp insertions in the A_7 run ($A_7 \rightarrow A_8$)**	**Complex mutations [a]**	**Other +1 frameshifts**
Wild type[b] (n=42)	**0.6 (0.5 – 1.2)**	**1**	**0.5 [1]**	**0.03**	**0.06**
msh2Δ (n=41)	**120 (88 – 150)**	**200**	**120 [240]**	**< 3**	**< 3**
rad27Δ (n=39)	**82 (66 – 110)**	**140**	**48 [96]**	**27**	**6**
msh2Δ rad27Δ (n=41)	**6,700 (5,900 – 9,400)**	**11,000**	**6,700 [13,400]**	**< 160**	**< 160**

The mutant strains are isogenic to E134 (wild type) and were obtained by dissection of tetrads of *MSH2/msh2Δ RAD27/rad27Δ* diploids. 95% confidence intervals are in parentheses and the relative rates of 1-bp insertions are in brackets. [a], each of the complex mutations consisted of an insertion and four or more other genetic alterations, all located within an ~20-bp DNA segment. [b], the wild-type data are from a previous report (42).

Table 3. Effect of deletion of *MSH2* and *RAD27* on *his7-2* mutation rate in the diploid *S. cerevisiae*

Genotype	***his7-2* mutation rate**		
	Absolute rate (x10^{-8})	**95% CI**	**Relative rate**
wild type	**0.9**	**0.7 – 1.3**	**1**
RAD27/rad27Δ MSH2/msh2Δ	**1.1**	**0.9 – 1.5**	**1**
RAD27/RAD27 msh2Δ/msh2Δ	**160**	**140 – 210**	**180**
rad27Δ/rad27Δ MSH2/MSH2	**200**	**150 – 230**	**220**
RAD27/rad27Δ msh2Δ/msh2Δ	**150**	**30 – 190**	**160**
rad27Δ/rad27Δ MSH2/msh2Δ	**610**	**320 – 860**	**680**
rad27Δ/rad27Δ msh2Δ/msh2Δ	**13,000**	**11,000 – 16,000**	**14,000**

The mutant diploid strains are derivatives of FKY1037 (wild type) and were prepared using the lithium acetate/PEG/DMSO transformation method.

Table 4. Effect of combining *msh2Δ* and *rad27Δ* on *lys2::InsE-A$_8$* mutation rate

Genotype	***lys2::InsE-A$_8$*** mutation rate	
	Absolute rate (x10^{-8})	**Relative rate**
wild type	**1.6 (1.4 – 4.2)**	**1**
msh2Δ	**750 (640 – 970)**	**460**
rad27Δ	**110 (76 – 160)**	**68**
msh2Δ rad27Δ	**21,000 (17,000 – 27,000)**	**13,000**

The strains are isogenic to E35 (wild type) and were prepared using the lithium acetate/PEG/DMSO transformation method. 95% confidence intervals are in parentheses.

Table 5. Effects of the different mutant combinations on *his7-2* mutation rate

Genotype	***his7-2* mutation rate**	
	Absolute rate (x10^{-8})	**Relative rate**
wild type	**0.7 (0.5 – 0.9)**	**1**
***msh3*Δ**	**2.3 (1.6 – 3.1)**	**3**
***msh6*Δ**	**3.0 (2.2 – 3.8)**	**4**
***msh3*Δ *msh6*Δ**	**110 [a] (93 – 140)**	**160**
***msh2*Δ**	**140 [a] (100 – 260)**	**200**
***rad27*Δ**	**46 (41 – 55)**	**66**
***msh2*Δ *rad27*Δ**	**6,800 [b, c] (4,500 – 9,900)**	**9,700**
***msh3*Δ *msh6*Δ *rad27*Δ**	**6,100 [d, e] (4,500 – 8,800)**	**8,800**
***msh3*Δ *rad27*Δ**	**91 (71 – 94)**	**130**
***msh6*Δ *rad27*Δ**	**520 (450 – 660)**	**740**
***mlh1*Δ**	**100 (88 – 130)**	**150**
***mlh1*Δ *rad27*Δ**	**3,500 [b, d] (2,500 – 5,100)**	**5,000**
***pms1*Δ**	**100 (72 – 120)**	**140**
***pms1*Δ *rad27*Δ**	**3,800 (2,500 – 4,300)**	**5,500**
pms1-E707K	**150 (110 – 230)**	**210**
***pms1-E707K rad27*Δ**	**3,900 [c, e] (2,600 – 5,100)**	**5,500**

The mutant haploid strains are isogenic to FKY688 (wild type) and were constructed using the lithium acetate/PEG/DMSO transformation method. 95% confidence intervals are in parentheses. [a], [b], [c], [d], and [e], the indicated mutation rates were analyzed by Mann-Whitney U two-tailed test. The two mutation rates marked [a] do not statistically differ from each other ([a]p=0.15). The difference between two mutation rates labeled with the same letter ([b],[c],[d] or [e]) is statistically significant ([b]p=0.008, [c]p=0.012, [d]p=0.01, and [e]p=0.021).

Table 6. Effects of *dna2-1 msh2*Δ on *his7-2* mutation rate

Genotype	***his7-2* mutation rate** [a]	
	Absolute rate (x10^{-8})	**Relative rate**
wild type	**0.8 (0.5 – 1.7)**	**1**
dna2-1	**8 (4 – 10)**	**10**
***msh2*Δ**	**120 (100 – 140)**	**160**
***dna2-1 msh2*Δ**	**280 (260 – 400)**	**340**

The strains are isogenic to E134 (wild type) and were prepared using the lithium acetate/PEG/DMSO transformation method. [a], the mutation rates were measured at 25°C. 95% confidence intervals are in parentheses.

Figure 1

A

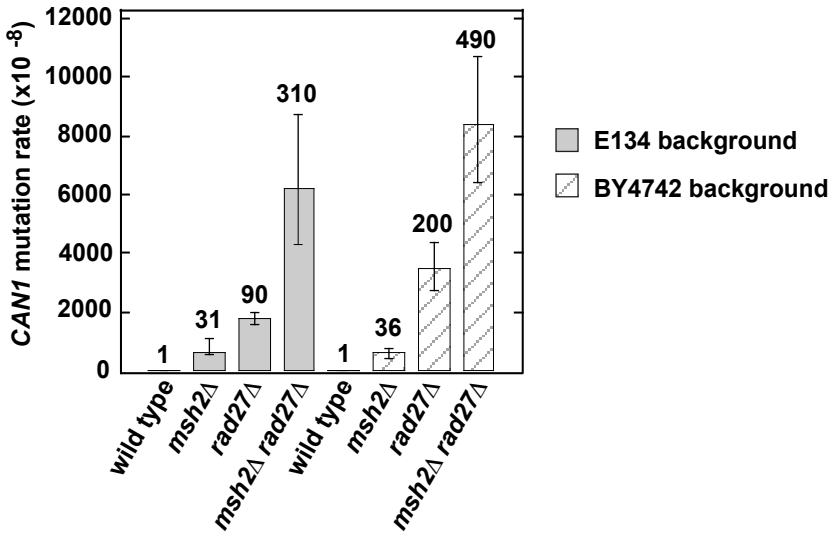

B

Genotype	Rates of indicated mutations (x 10^{-8})						
	1-bp insertions[a]	Base substitutions	1-bp deletions	Duplications (6-14 bp)	Duplications (17-416 bp)	Other mutations	Total
Wild type (n=43)	1.4 (1)	17 (1)	1.4 (1)	< 0.5	< 0.5	0.5	20
*rad27*Δ (n=47)	115 (82)	77 (5)	38 (27)	< 38	1,500	77	1,800
*msh2*Δ (n=48)	51 (36)	210 (12)	360 (260)	< 13	< 13	< 13	620
*msh2*Δ *rad27*Δ (n=49)	2,000 (1,400)	380 (22)	630 (450)	630	2,400	< 130	6,200

Figure 2

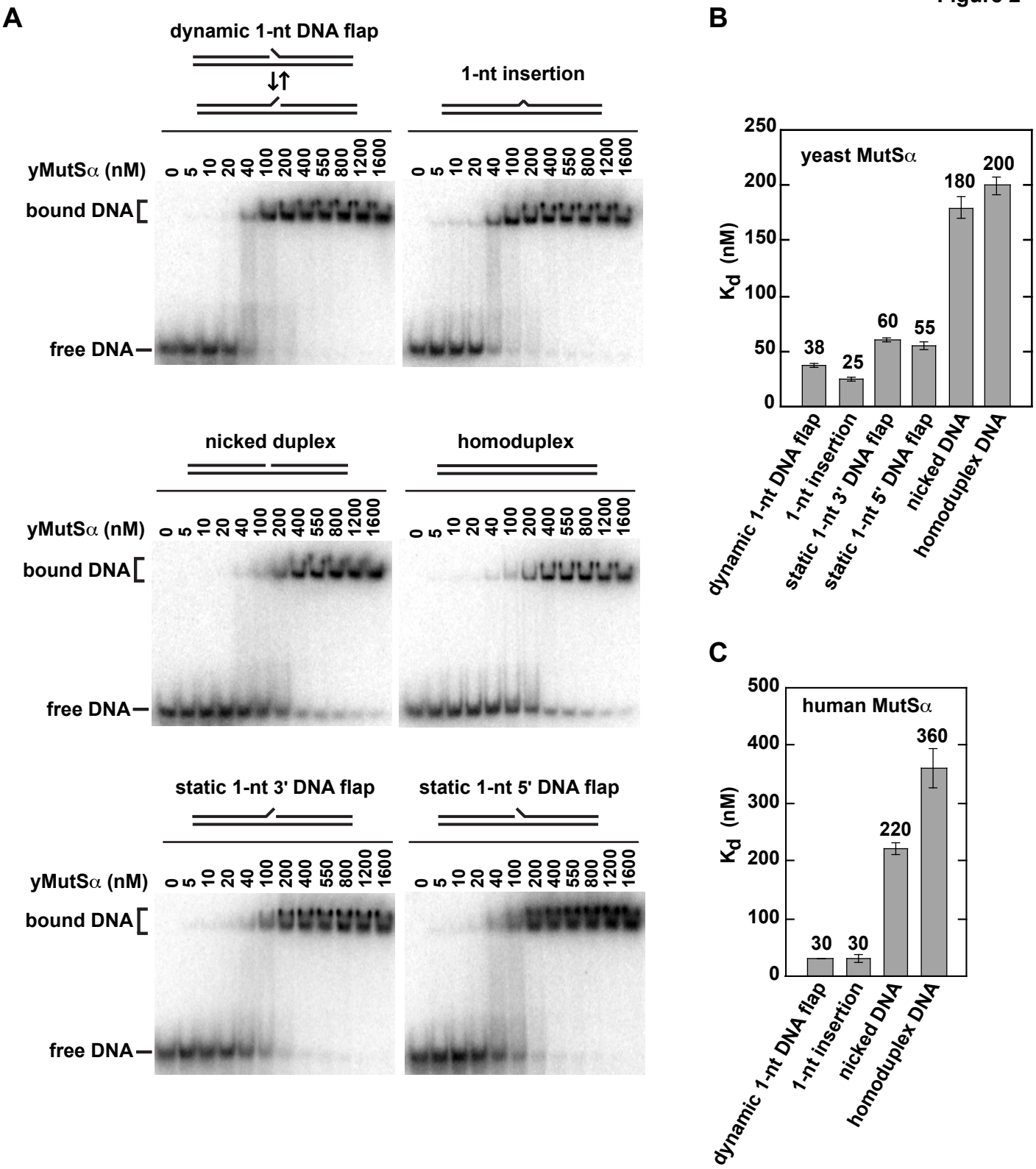
A
dynamic 1-nt DNA flap
1-nt insertion
nicked duplex
homoduplex
static 1-nt 3' DNA flap
static 1-nt 5' DNA flap
yMutSα (nM)
0 5 10 20 40 100 200 400 550 800 1200 1600
bound DNA
free DNA
B
yeast MutSα
Kd (nM)
250
200
150
100
50
0
38
25
60
55
180
200
dynamic 1-nt DNA flap
1-nt insertion
static 1-nt 3' DNA flap
static 1-nt 5' DNA flap
nicked DNA
homoduplex DNA
C
human MutSα
Kd (nM)
500
400
300
200
100
0
30
30
220
360
dynamic 1-nt DNA flap
1-nt insertion
nicked DNA
homoduplex DNA

Figure 3

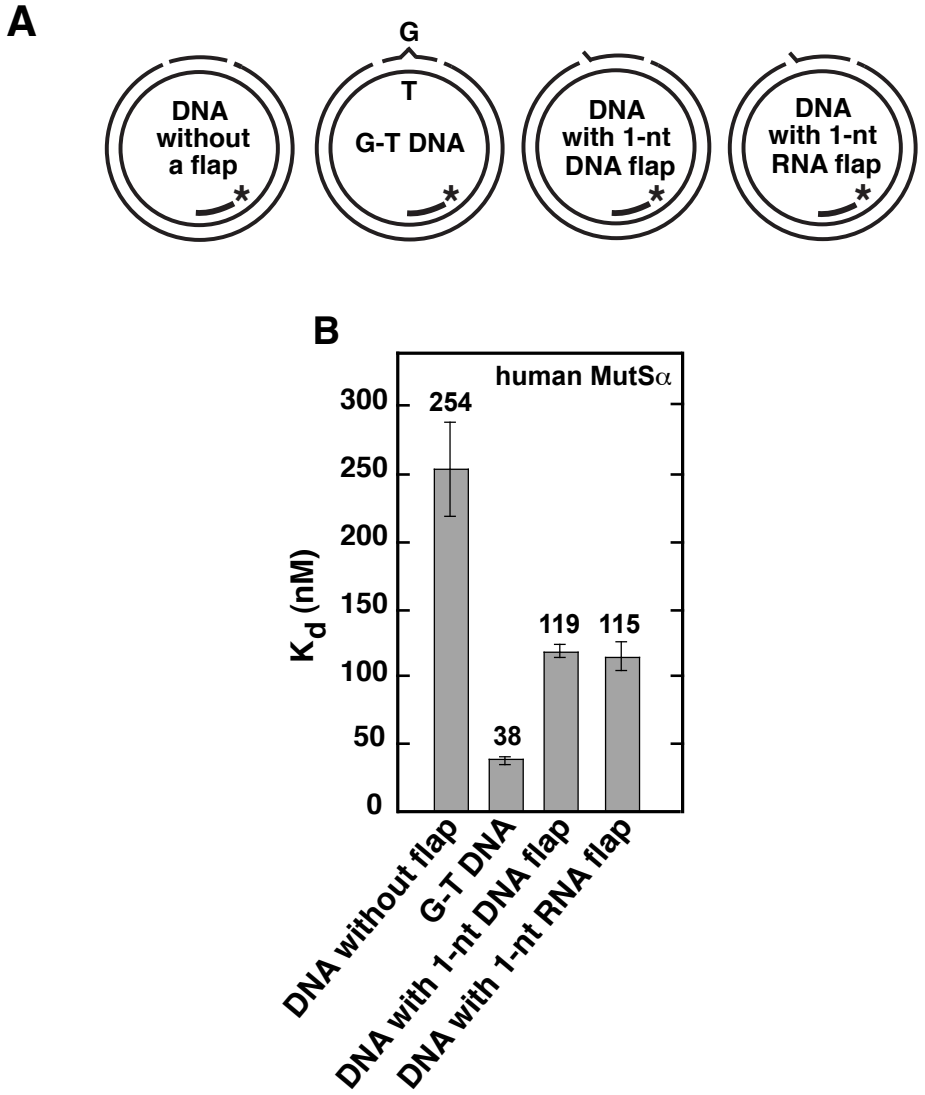
A
G
T
DNA without a flap
G-T DNA
DNA with 1-nt DNA flap
DNA with 1-nt RNA flap
B
human MutSα
K_d (nM)
300
250
200
150
100
50
0
254
38
119
115
DNA without flap
G-T DNA
DNA with 1-nt DNA flap
DNA with 1-nt RNA flap

A

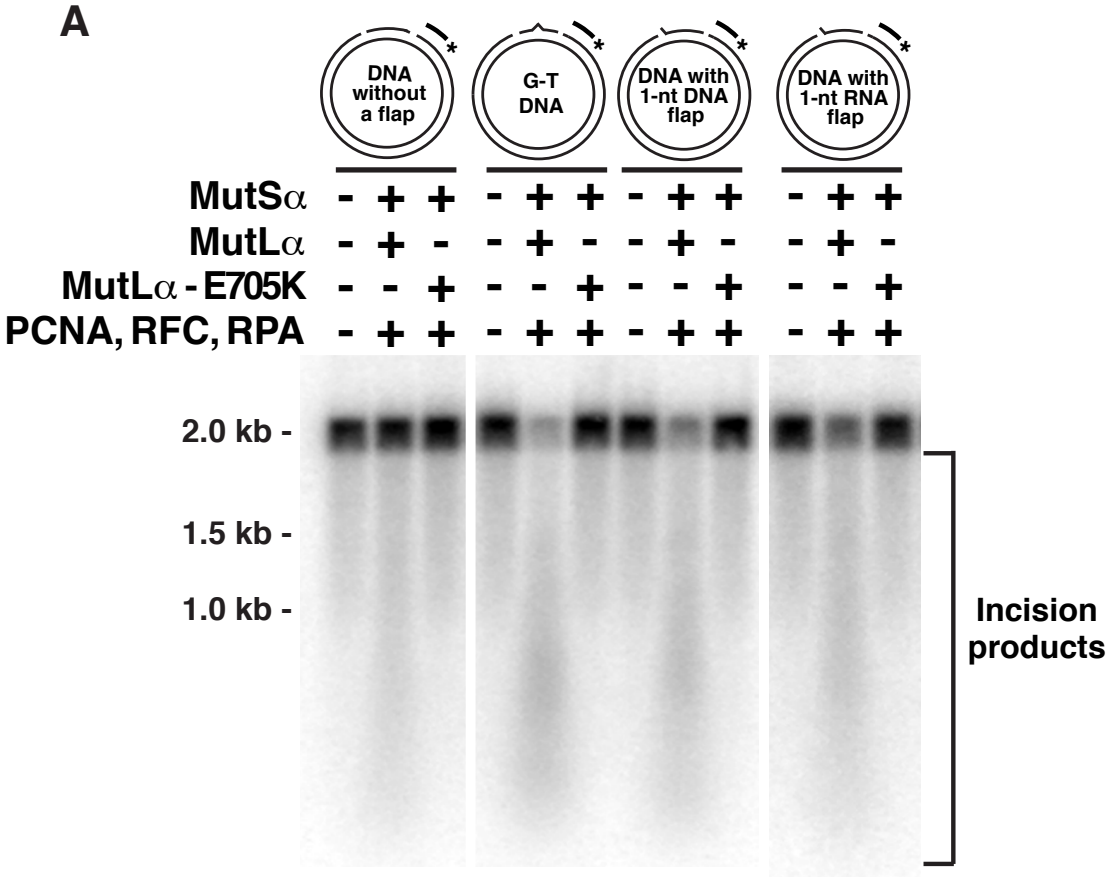

B

Protein mixture	Incision (%)			
	DNA without a flap	G-T DNA	DNA with 1-nt DNA flap	DNA with 1-nt RNA flap
MutLα, MutSα, PCNA, RFC, RPA	10 ± 2	48 ± 2	34 ± 5	30 ± 1
MutLα-E705K, MutSα, PCNA, RFC, RPA	2 ± 2	1 ± 1	2 ± 1	0 ± 1

Figure 5

A

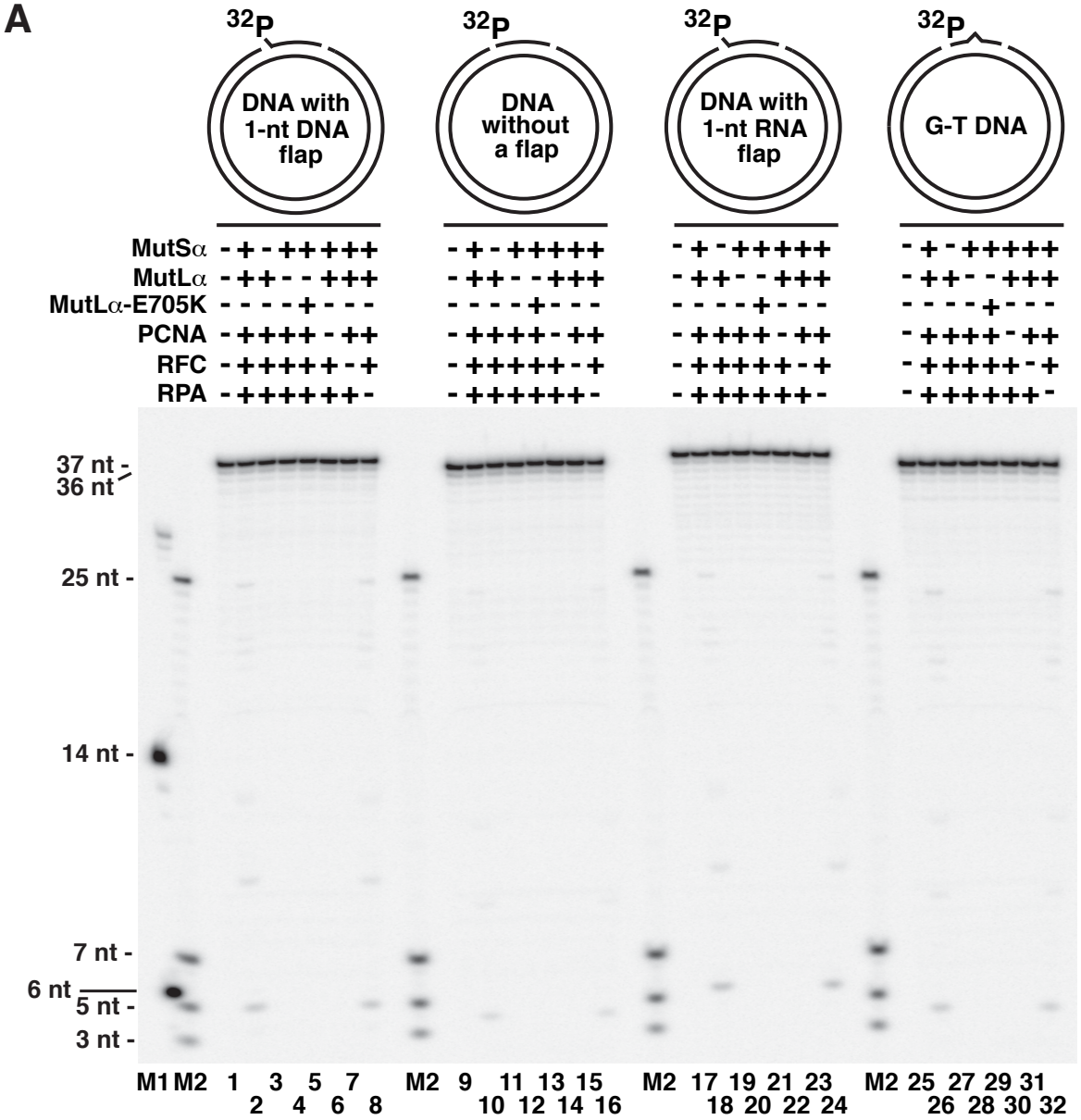

B

Protein mixture	Incision (%)			
	DNA with 1-nt DNA flap	DNA without a flap	DNA with 1-nt RNA flap	G-T DNA
complete (MutLα, MutSα, PCNA, RFC, & RPA)	4.5 ± 0.8	1.5 ± 0.3	5.4 ± 0.5	2.8 ± 0.6
- MutSα	< 0.1	< 0.1	< 0.1	< 0.1
- MutLα	< 0.1	< 0.1	< 0.1	< 0.1
- MutLα, + MutLα-E705K	< 0.1	< 0.1	< 0.1	< 0.1
- PCNA	< 0.1	< 0.1	< 0.1	< 0.1
- RFC	< 0.1	< 0.1	< 0.1	< 0.1
- RPA	3.8 ± 0.2	1.3 ± 0.2	4.6 ± 0.7	2.6 ± 0.6

C

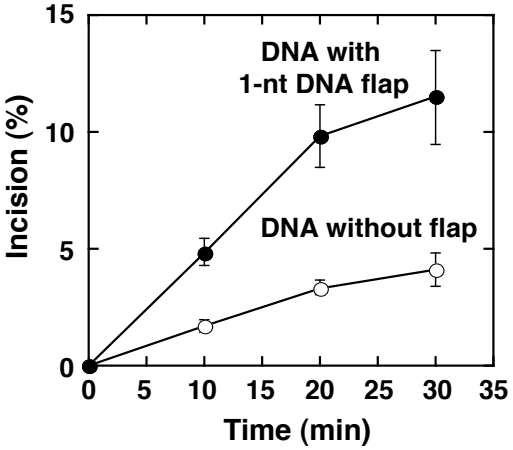

Figure 6

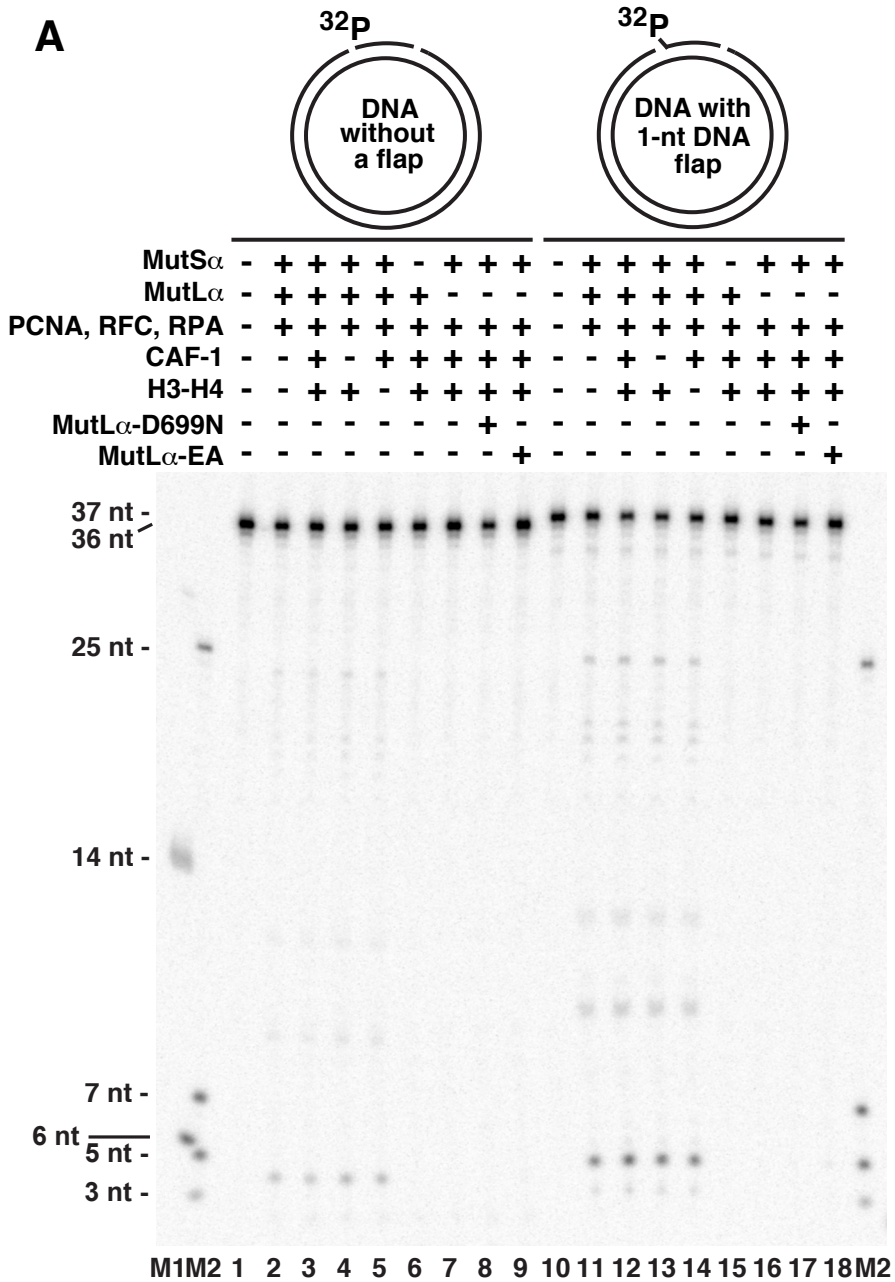
A
32P
DNA without a flap
32P
DNA with 1-nt DNA flap
MutSα - + + + + - + + + - + + + + - + + +
MutLα - + + + + + - - - - + + + + + - - -
PCNA, RFC, RPA - + + + + + + + + - + + + + + + + +
CAF-1 - - + - + + + + + - - + - + + + + +
H3-H4 - - + + - + + + + - - + + - + + + +
MutLα-D699N - - - - - - - + - - - - - - - - + -
MutLα-EA - - - - - - - - + - - - - - - - - +
37 nt -
36 nt
25 nt -
14 nt -
7 nt -
6 nt
5 nt -
3 nt -
M1 M2 1 2 3 4 5 6 7 8 9 10 11 12 13 14 15 16 17 18 M2

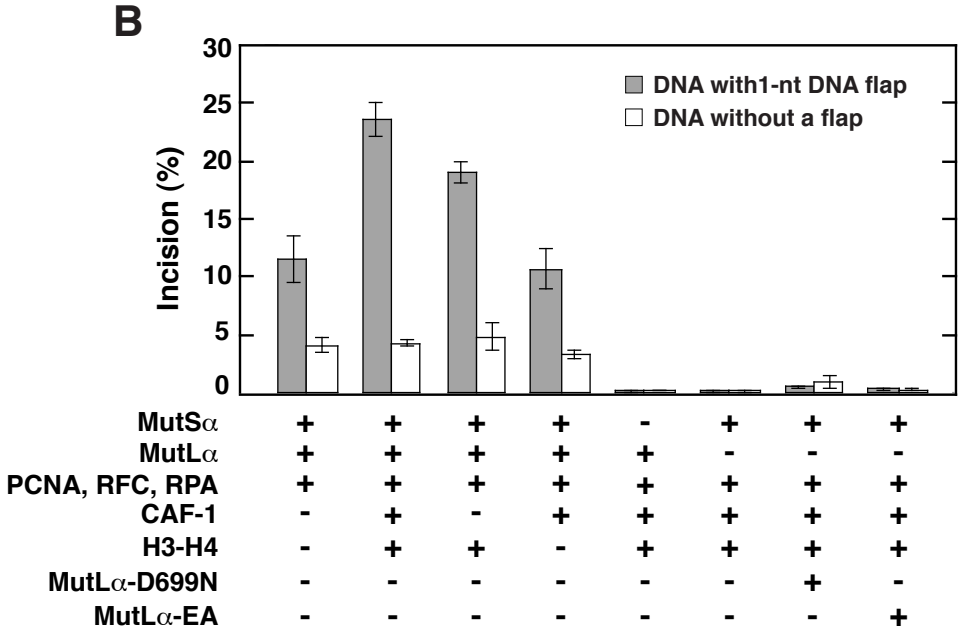
B
Incision (%)
30
25
20
15
10
5
0
DNA with1-nt DNA flap
DNA without a flap
MutSα + + + + - + + +
MutLα + + + + + - - -
PCNA, RFC, RPA + + + + + + + +
CAF-1 - + - + + + + +
H3-H4 - + + - + + + +
MutLα-D699N - - - - - - + -
MutLα-EA - - - - - - - +

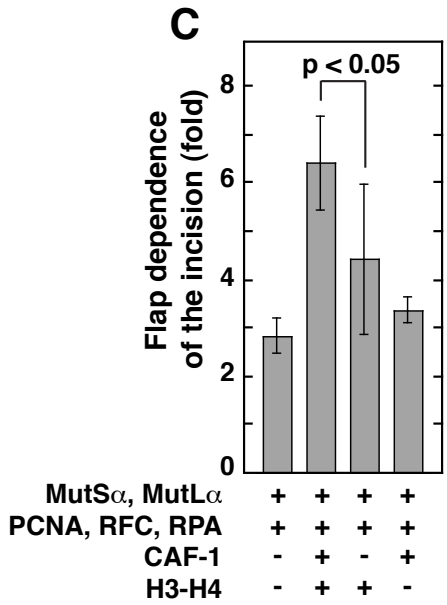
C
p < 0.05
Flap dependence of the incision (fold)
8
6
4
2
0
MutSα, MutLα + + + +
PCNA, RFC, RPA + + + +
CAF-1 - + - +
H3-H4 - + + -

Figure 7

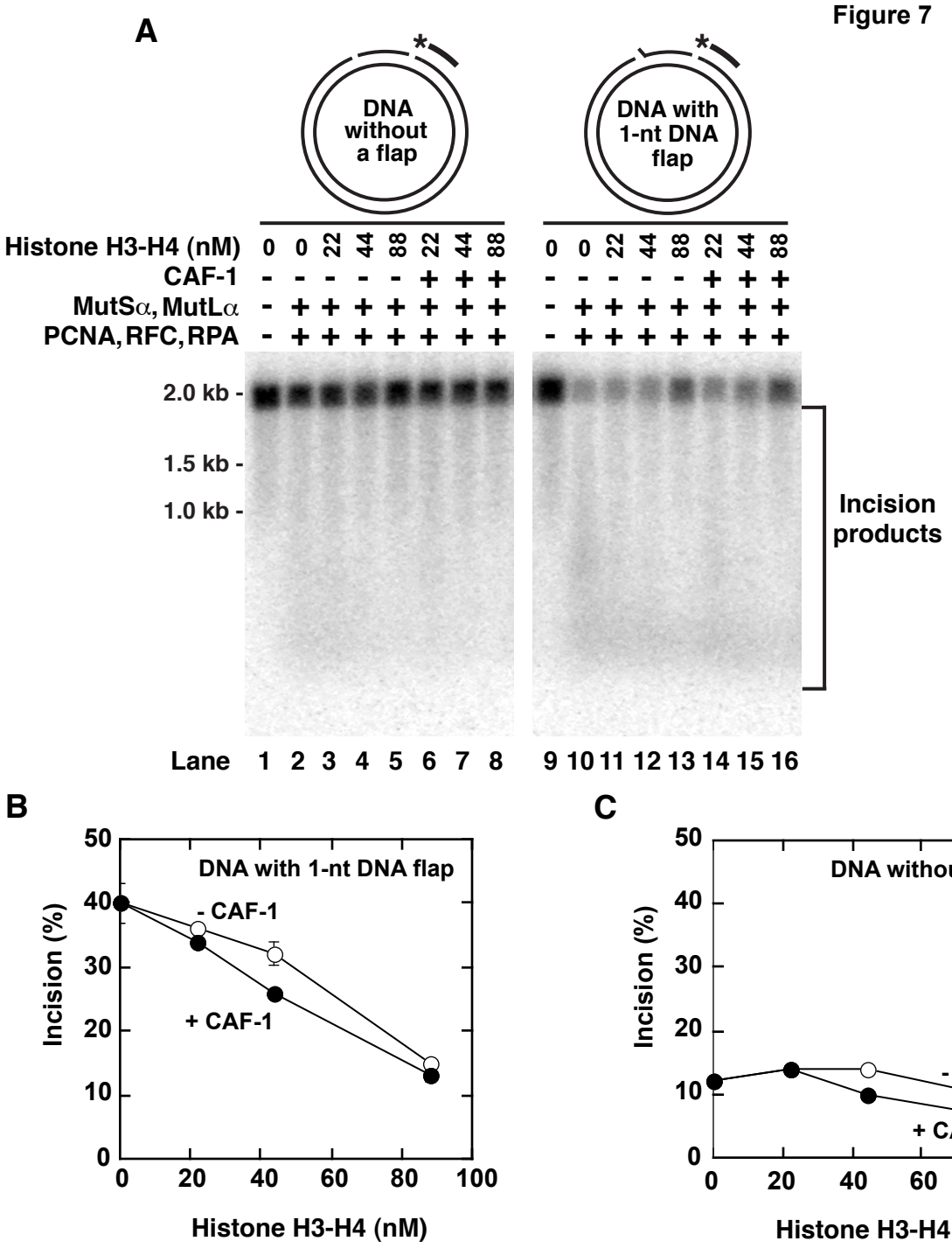
A
DNA without a flap
DNA with 1-nt DNA flap
Histone H3-H4 (nM) 0 0 22 44 88 22 44 88 0 0 22 44 88 22 44 88
CAF-1 - - - - - + + + - - - - - + + +
MutSα, MutLα - + + + + + + + - + + + + + + +
PCNA, RFC, RPA - + + + + + + + - + + + + + + +
2.0 kb -
1.5 kb -
1.0 kb -
Incision products
Lane 1 2 3 4 5 6 7 8 9 10 11 12 13 14 15 16
B
DNA with 1-nt DNA flap
- CAF-1
+ CAF-1
Incision (%)
Histone H3-H4 (nM)
C
DNA without a flap
- CAF-1
+ CAF-1
Incision (%)
Histone H3-H4 (nM)

Figure 8

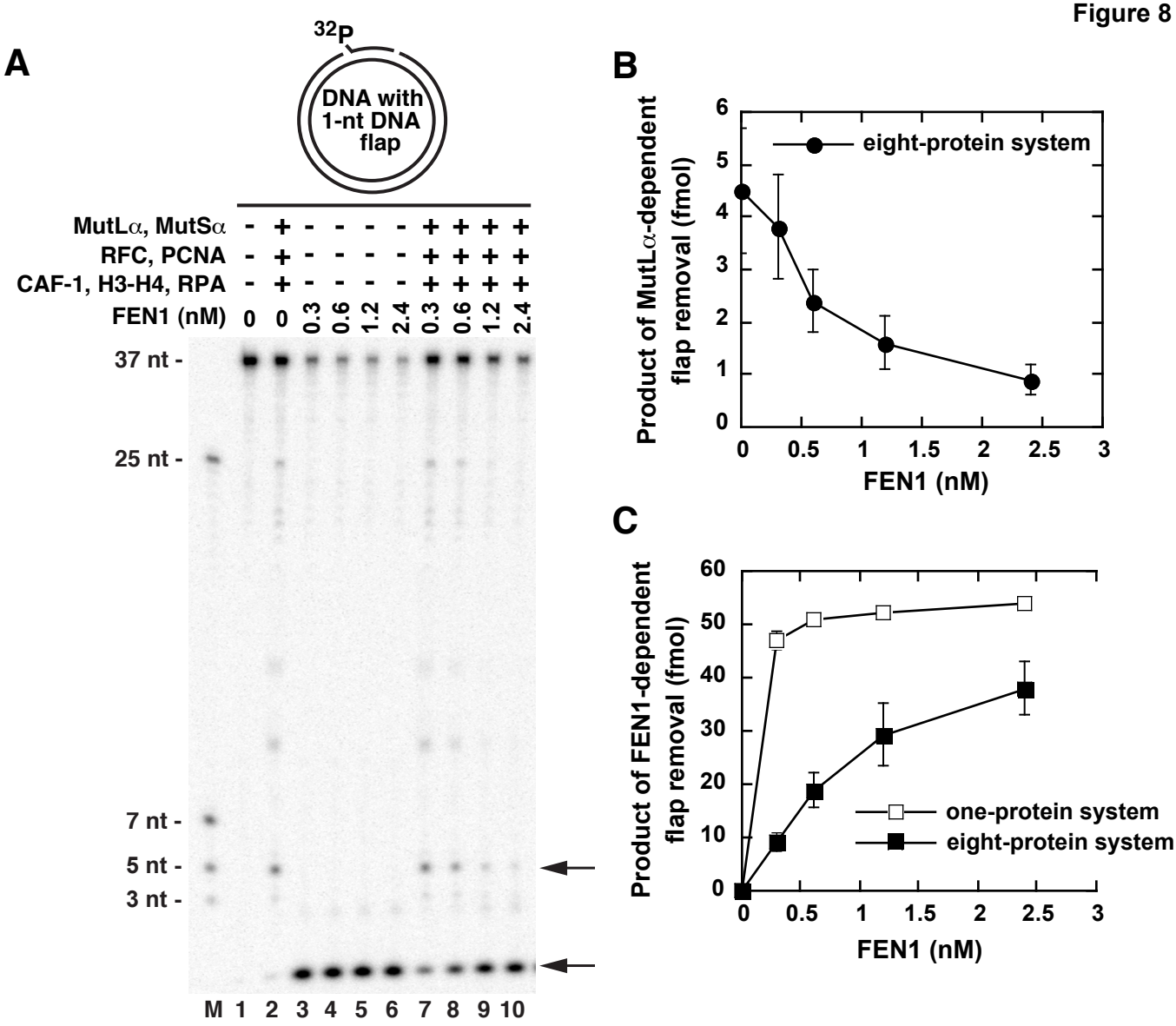
A
32P
DNA with 1-nt DNA flap
MutLα, MutSα - + - - - - + + + +
RFC, PCNA - + - - - - + + + +
CAF-1, H3-H4, RPA - + - - - - + + + +
FEN1 (nM) 0 0 0.3 0.6 1.2 2.4 0.3 0.6 1.2 2.4
37 nt -
25 nt -
7 nt -
5 nt -
3 nt -
M 1 2 3 4 5 6 7 8 9 10
B
eight-protein system
Product of MutLα-dependent flap removal (fmol)
FEN1 (nM)
C
one-protein system
eight-protein system
Product of FEN1-dependent flap removal (fmol)
FEN1 (nM)

Figure 9

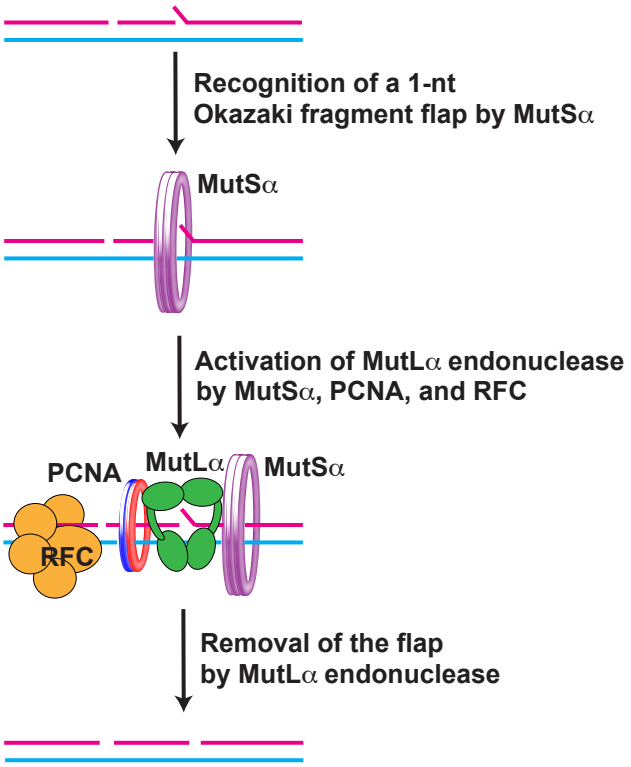
Recognition of a 1-nt
Okazaki fragment flap by MutSα
MutSα
Activation of MutLα endonuclease
by MutSα, PCNA, and RFC
PCNA
MutLα
MutSα
RFC
Removal of the flap
by MutLα endonuclease